I&EC research
Industrial & Engineering Chemistry Research

REVIEW

pubs.acs.org/IECR

Preparation and Characterization of Membranes Formed by Nonsolvent Induced Phase Separation: A Review

Gregory R. Guillen, Yinjin Pan, Minghua Li, and Eric M. V. Hoek*

Department of Civil and Environmental Engineering, California NanoSystems Institute, University of California, Los Angeles, California 90095, United States

ABSTRACT: The methods and mechanisms of nonsolvent induced phase separation have been studied for more than fifty years. Today, phase inversion membranes are widely used in numerous chemical industries, biotechnology, and environmental separation processes. The body of knowledge has grown exponentially in the past fifty years, which suggests the need for a critical review of the literature. Here we present a review of nonsolvent induced phase separation membrane preparation and characterization for many commonly used membrane polymers. The key factors in membrane preparation discussed include the solvent type, polymer type and concentration, nonsolvent system type and composition, additives to the polymer solution, and film casting conditions. A brief introduction to membrane characterization is also given, which includes membrane porosity and pore size distribution characterization, membrane physical and chemical properties characterization, and thermodynamic and kinetic evaluation of the phase inversion process. One aim of this review is to lay out the basics for selecting polymer−solvent−nonsolvent systems with appropriate film casting conditions to produce membranes with the desired performance, morphology, and stability, and to choose the proper way to characterize these properties of nonsolvent induced phase inversion membranes.

1. INTRODUCTION

Filtration is the process through which a solid component is separated from a fluid stream primarily based on differences in size between particles and fluid. Usually filtration refers to the separation of particulate matter from a liquid or gaseous stream.[1] Membrane filtration extends the range of solid−liquid separations to colloidal particles, macromolecules, and dissolved solutes for selective separation of gas mixtures and multicomponent solutions.[2] For molecular separations, membranes offer numerous advantages such as (1) not requiring a phase change for solute or the carrier solvent; (2) excellent combination of selectivity and productivity; and (3) no need for regeneration of solid or liquid sorbents. As such, membranes are widely used in many important chemical, biological, and environmental applications.

Many kinds of synthetic materials can be used for preparing membranes such as ceramics, glasses, metals, or polymers. The aim is to prepare the material to obtain a membrane structure with morphology tailored for a specific separation. A number of preparation techniques exist such as sintering, stretching, track-etching, template-leaching, and dip-coating, which enable a membrane to be constructed from a given material and with the desired membrane morphology.[3] Phase inversion techniques are among the most important and commonly used processes for preparing membranes from a large number of polymeric building blocks. Publications on phase inversion increased exponentially in the past fifty years (Figure 1).

An asymmetric membrane with a very thin, dense skin layer can be prepared by either dry or wet phase inversion processes, such as solvent evaporation, precipitation from the vapor phase, precipitation by controlled evaporation, thermal precipitation, and immersion precipitation.[3] Of all these techniques, immersion precipitation is among the first to be commercially explored and is one of the most popular membrane formation methods because it allows for the preparation of many membrane morphologies.

Development of integrally skinned asymmetric membranes by Loeb and Sourirajan in the 1960s is a major breakthrough in membrane technology.[4] In their research, the phase inversion method was employed to transform a polymer in a controlled manner from a liquid dispersion to a solid film. Over the past half century, a plethora of knowledge has been generated about phase inversion membranes formed by immersion precipitation, also known as nonsolvent induced phase inversion.

Generally, flat sheet membranes are formed by coating a porous mechanical support with a thin film of polymer solution. The polymer solution, or dope, is composed of at least one polymer, at least one good solvent, and may contain additives. The thin film and support are immersed into a coagulation bath, which consists of a poor solvent, i.e., the nonsolvent, and may contain additives. The polymer film solidifies through exchange of the solvent and nonsolvent; hence, the solvent−nonsolvent system must be miscible.[5,6] The tubular form is the alternative geometry for a membrane, including hollow fiber membranes (diameter <0.5 mm), capillary membranes (0.5 mm < diameter <5 mm), and tubular membranes (diameter >5 mm).[3] Tubular membranes usually have large dimensions and must be supported, whereas hollow fibers and capillaries are self-supported. Hollow fibers and capillaries can be prepared via three different methods: wet spinning, melt spinning, and dry spinning. Spinning parameters and fiber dimensions are very important with respect to membrane performance.[7−10]

Different separation processes require membranes with specific physical and chemical properties as described in Table 1. To produce a membrane with suitable chemical stability and permeation properties, some key factors for the casting solution system

Received: September 19, 2010
Accepted: February 3, 2011
Revised: January 28, 2011
Published: March 08, 2011

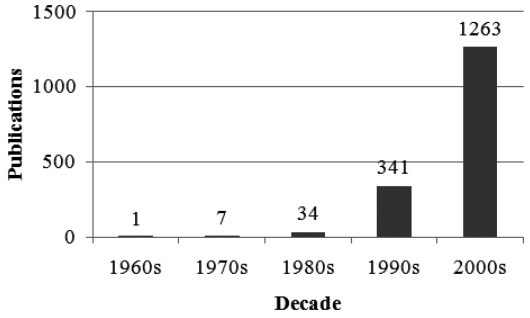

Figure 1. Publications on phase inversion membranes in *Web of Knowledge*.

should be considered. The key factors that influence phase inversion membrane formation include the choice of solvent−nonsolvent system, the composition of the polymer solution, the composition of the coagulation bath, and film casting conditions.[11] In this paper, we review these factors for nonsolvent induced phase separation membrane preparation and characterization for the most common membrane polymers.

2. MECHANISMS OF NONSOLVENT INDUCED PHASE INVERSION

In early research, Strathmann et al. used the ternary phase diagram to discuss the thermodynamic aspects of instantaneous demixing and delayed demixing processes, which lead to different types of membrane structures.[12] This phase diagram can conveniently be used to analyze the thermodynamics of the membrane precipitation process. Typical phase diagrams are shown schematically in Figure 2. The corners of the triangle represent the three components (polymer, solvent, and nonsolvent), while any point within the triangle represents a mixture of three components. The system consists of two regions: a one-phase region where all components are miscible and a two-phase region where the system separates into polymer-rich and polymer-poor phases. The line which connects a pair of equilibrium compositions in the phase diagram is called a tie line. The liquid−liquid phase boundary is the so-called binodal. Every composition inside the binodal curve will demix into two liquid phases which differ in composition but which are in thermodynamic equilibrium with each other. Wijmans et al. elaborated two ways, including a rapid titration method and a turbidity measurement method, to measure the cloud point in order to determine the binodal.[13]

Using this ternary phase diagram, the composition path of a polymer film can be expressed schematically at a certain time of immersion in a nonsolvent bath.[3] From Figure 2a it can be seen that at $t < 1$ s, the composition path crosses the binodal line, which means liquid−liquid demixing starts immediately after immersion. Figure 2b shows that all compositions directly beneath the top layer remain in the one-phase region and are still miscible, which means no demixing occurs immediately after immersion. After a longer time interval, compositions beneath the top layer will cross the binodal and demixing will also start in this case. Thus two distinctly different demixing processes can be distinguished and the resulting membrane morphologies are also completely different.[3,14] Strathmann et al. also observed these two fundamentally different structures depending on the rate of polymer precipitation by nonsolvent induced phase separation.[15] Precipitation rate is measured as the time between immersing the casting solution in a precipitation bath and the time when that solution turns opaque or when the membrane separates from the glass plate. Their research showed that slow precipitation rates produced membranes with "sponge-like" morphologies. These membranes usually had high salt rejections and low water fluxes when tested as reverse osmosis membranes. Fast precipitation rates produced membranes with large "finger-like" macrovoids in the substructure. These membranes had low salt rejections and high water fluxes. In general, changes in membrane formation chemistry or casting conditions that slow down the rate of precipitation tend to produce a membrane with sponge-like morphology, low flux, and high solute rejection.

A mass transfer model for the early stages of the phase inversion process was developed by Cohen et al.[16] They created a model for the diffusion-controlled formation of porous membranes obtained by nonsolvent induced phase separation. It was assumed that when phase separation occurs, a three-dimensional structure consisting of two interspersed equilibrium phases will form. This two-phase structure will then spread to all compositions below the binodal. It was also assumed that solvent and nonsolvent diffusion coefficients are equal, so the flow of solvent and nonsolvent in the film can be treated as a one-dimensional diffusion process as shown in Figure 3. At time t a propagating diffusion layer bounded on one side by the nonsolvent bath and on the other by casting solution has developed. With their diffusion model they also confirmed the exchange of solvent and nonsolvent could lead to unstable compositions in the polymer solution.

Following Cohen's work, Reuvers et al.,[17] Tsay et al.,[18] and Radovanovic et al.[19,20] predicted precipitation paths. The model built by Radovanovic et al.[19] was frequently used to describe mass transfer phenomena occurring during the immersion step. Using the continuity equation (eq 1) a set of general diffusion equations and boundary conditions have been derived for the mass transport in a ternary polymer solution after immersion into a coagulation bath and prior to demixing process

$$\frac{\partial(\phi_i/\phi_3)}{\partial t} = \frac{\partial J_i^p}{\partial m},\ i = 1,2 \tag{1}$$

where m is the position coordinate in the polymer-fixed frame of reference and is defined as

$$m(z,t) = \int_0^z \phi_3(x,t)\mathrm{d}x \tag{2}$$

Here J_i^p is the volume flux of component i, ϕ_i is the volume fraction of component i, t is time, i = 1, 2, 3 represents the nonsolvent, solvent, and polymer, respectively. Initial concentrations are assumed constant

$$\phi_i(m,0) = \phi_i^o,\ i = 1,2 \tag{3}$$

After immersion, the following boundary conditions exist:

$$\phi_i(0,t) = \phi_i^s,\ i = 1,2 \tag{4}$$

$$\phi_i(\infty,t) = \phi_i^o,\ i = 1,2 \tag{5}$$

where ϕ_i^s is the volume fraction of component i that is in equilibrium with the coagulation bath at the film−bath interface. Fluxes in the polymer-fixed reference frame are related to component velocities, v_i, by

$$J_i^p = \frac{1-\phi_j}{\phi_3}\phi_i v_i + \frac{\phi_i}{\phi_3}\phi_j v_j,\ i,j = 1,2,\ i \neq j \tag{6}$$

dx.doi.org/10.1021/ie101928r |*Ind. Eng. Chem. Res.* 2011, 50, 3798–3817

Table 1. Desirable Phase-Inversion Membrane Material Properties by Application[2,3,116,199−214]

membrane type		desirable properties	applications	ref
MF	physical morphology	thin, porous skin layer with narrow pore size distribution (0.05−10 μm)	sterile filtration of pharmaceuticals, cell harvesting, clarification of fruit juice/wine/beer, ultapure water, metal recovery as colloidal orhydroxides, water-wastewater treatment, fermentation, separation of oil−water emulsions	3,116,199−203
	chemical properties	chemical stability over a wide pH range; mechanically and thermally stable		
UF	physical morphology	porous skin layer; asymmetric structure; much denser top layer than MF membranes; pore size (0.5 um−l nm) (lower limit a few thousand Dalton); macro void morphology: finger-like, sponge-like	food and dairy industry, pharmaceutical industry, textile industry, chemical industry, metallurgy, paper industry, water treatment	2,3,116,201
	chemical properties	good chemical, mechanical, and thermal stability; low fouling tendency		
NF & RO	physical morphology	thin dense toplayer and porous sublayer; pore size <2 nm; good thermal and mechanical stability; higher membrane resistance for higher pressure, tensile strength	desalination, removal of micropollutants, water softening, wastewater treatment, retention of dyes (textile industry), ultrapure water (electronic industry), concentration of food, juice, and sugars (food industry), concentration of milk (dairy industry)	3,116,204−207
	chemical properties	good chemical and thermal stability; hydrophilic; antifouling		
gas separation	physical morphology	porous/nonporous, asymmetric/composite membrane; elastometric/glassy polymeric toplayer; selectivity as important as permeability; permeable top layer, defect-free; thin (0.1 to few μm); open porous support layer for mechanical support for toplayer (minimize resistance); no macro voids	removal of H_2O, organic vapors from air, dehydration (compressed air, natural gas, air conditioning), acid gases from flue gas	3,116,208,209
	chemical properties	chemically stable in separation gas (such as Cl_2)		
pervaporation and vapor permeation	physical morphology	nonporous membrane; thickness should be 0.1 to few μm for toplayer; anisotropic morphology: dense toplayer, open porous sublayer; narrow pore size distribution, no macrovoids	dehydration of organic solvent, removal of organic components from water (alcohols, aromatics, chlorinated hydrocarbons), separation of polar/nonpolar (e.g., alcohols/aliphatics), separation of saturated/unsaturated (e.g., cyclohexane/benzene), separation of isomers	3,116,206,210,211
	chemical properties	stable in vapor and solvent		
dialysis	physical morphology	minimize thickness (10−100 μm)	hemodialysis (removal of toxic substance from blood), alchohol reduction in beer, desalination of enzymes and coenzymes, alkai recovery in pulp and paper industry	3,116,200,212
	chemical properties	hydrophilic polymers for aqueous application, blood compatibility for hemo dialysis		
membrane distillation	physical morphology	symmetric or asymmetric; porous, thickness should be 0.2−1.0 μm; high porosity with pore size in the range of 0.2−0.3 μm; no macrovoids	pure water production, labortories, semiconductors industry, desalination, production of boiler feedwater, concentration of aqueous solution, removal of VOCs, contaminated surface water (benzene, TCE), fermentation products (ethanol, butanol), aroma compounds	3,116,213
	chemical properties	very hydrophobic materials, liquid must not wet membrane		
forward osmosis and pressure retarded osmosis	physical morphology	dense active layer for high solute rejection; porous support for higher water flux; high mechanical strength, highly ordered, open, interconnected finger-like voids to promote internal mass transfer	wastewater treatment and water purification, desalination, food processing, pharmaceutical industry, osmotic pumps, osmotic power, pressure-retarded osmosis	3,116,214
	chemical properties	very hydrophilic to enhance flux and reduce membrane fouling		

dx.doi.org/10.1021/ie101928r |Ind. Eng. Chem. Res. 2011, 50, 3798–3817

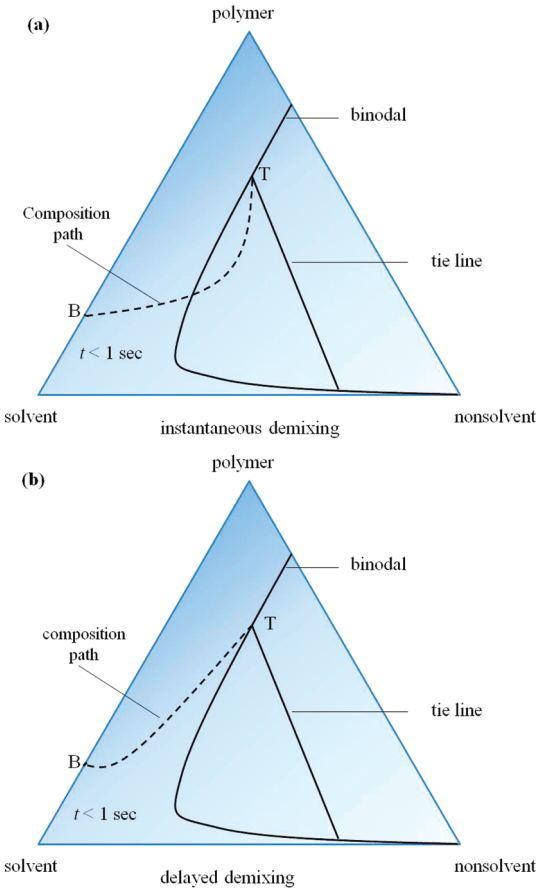

Figure 2. Composition paths of a cast film immediately after immersion (t < 1 s) demonstrating (a) instantaneous demixing and (b) delayed demixing; T and B represent top and bottom of the film, respectively.[3]

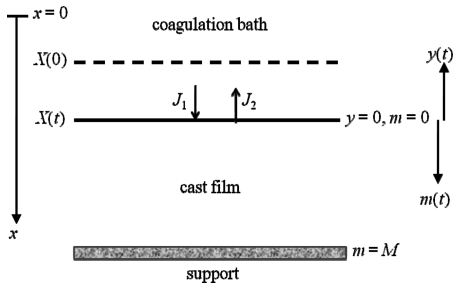

Figure 3. Flow of solvent and nonsolvent treated as a one-dimensional diffusion process and coordinate systems for membrane formation model.[17,19]

Component fluxes are related to chemical potentials, μ_i, by

$$\frac{1}{RT}\frac{\partial \mu_i}{dz} = \sum_{j=1}^{3} \phi_j \xi_{ij}(v_j - v_i),\ i = 1,3 \tag{7}$$

where ξ_{ij} is a frictional coefficient between components i and j. A modified flux is defined as

$$N_i = J_i^p t^{1/2},\ i = 1,2 \tag{8}$$

along with a new variable

$$\eta = mt^{-1/2} \tag{9}$$

Equation 1 simplifies to the ordinary differential equation

$$\eta\frac{\mathrm{d}(\phi_i/\phi_3)}{\mathrm{d}t} + 2\frac{\mathrm{d}N_i}{\mathrm{d}\eta} = 0 \tag{10}$$

with new boundary conditions of

$$\phi_i(0) = \phi_i^s,\ i = 1,2 \tag{11}$$

$$\phi_i(\infty) = \phi_i^o,\ i = 1,2 \tag{12}$$

Equation 7 transforms to

$$N_i = -\sum_{j,k}^{2} F_{ij}T_{jk}\frac{d\phi_k}{d\eta},\ i = 1,2 \tag{13}$$

where F_{ij} and T_{jk} are frictional and thermodynamic contributions which are defined by Radovanovic et al.[19]

Diffusion in the coagulation bath is described by

$$\frac{\partial v_i}{\partial t} = \frac{\partial}{\partial y}\left(D\frac{\partial v_i}{\partial y}\right) - \frac{\partial v_i}{\partial y}\frac{\mathrm{d}X}{\mathrm{d}t} \tag{14}$$

$$\frac{\mathrm{d}X}{\mathrm{d}t} = -J_1^p(0,t) - J_2^p(0,t) \tag{15}$$

where v_i is the volume fraction of component i in the coagulation bath, X is the position of the interface between the film and the coagulation bath, x is the spatial position coordinate normal to the membrane surface, $y = -x + X(t)$ is the position coordinate that moves with the interface. Initial and boundary conditions for the nonsolvent are

$$v_1(y,0) = v_1^o \tag{16}$$

$$v_1(0,t) = v_1^s \tag{17}$$

$$v_1(\infty,t) = v_1^o \tag{18}$$

By defining a new variable

$$\theta = yt^{-1/2} \tag{19}$$

equation 14 transforms to

$$\frac{\partial v_1}{\partial \theta} = -\frac{2}{\theta}\left\{[N_1(0) + N_2(0)]\frac{\mathrm{d}v_1}{\mathrm{d}\theta} + \frac{d}{\mathrm{d}\theta}\left(D\frac{\mathrm{d}v_1}{\mathrm{d}\theta}\right)\right\} \tag{20}$$

with boundary conditions

$$v_1(0) = v_1^s \tag{21}$$

$$v_1(\infty) = v_1^o \tag{22}$$

The mutual diffusion coeffiecient, D, is concentration dependent and defined by Radovanovic et al.[19]

The diffusion model explained the two types of demixing taking place during the phase inversion process and was used to predict the range of the initial composition of the casting film. To calculate the critical initial compositions at which the demixing changes from instantaneous to delayed, the diffusion equation for the film (eq 10) and for the bath (eq 20) must be solved simultaneously.[19] When from solving eq 10, the composition profile touches or crosses the binodal line (Figure 2a), instantaneous demixing will happen which means the polymer precipitates and a solid film is formed very rapidly after immersion in the nonsolvent bath. This type of

dx.doi.org/10.1021/ie101928r |Ind. Eng. Chem. Res. 2011, 50, 3798–3817

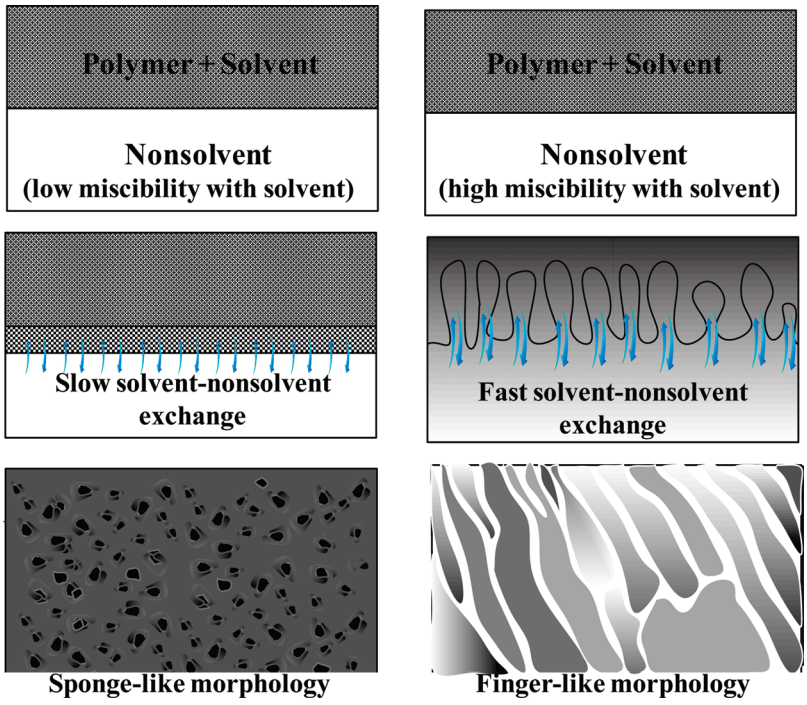

Figure 4. Different membrane morphologies caused of different types of demixing.

demixing generally shows a highly porous substructure (with finger-like macrovoids) and finely porous, thin skin layers. If the composition profile does not touch the binodal line (Figure 2b), demixing is delayed, precipitation is slow, and it takes much longer for the membrane to form. Membranes with a relatively dense top layer and sponge-like substructure are obtained. The structures of these two types of membrane are shown in Figure 4.

Asymmetric membranes consist of a thin top layer supported by a porous sublayer that often contain large void spaces, or macrovoids. These macrovoids may exhibit different morphologies (i.e., finger-like or sponge-like) depending on phase inversion kinetics and thermodynamics. See discussion below for more detail about macrovoid formation and morphology. The presence of macrovoids in membranes has both advantages and disadvantages. Macrovoids could result in compaction or collapse of membranes and therefore limit the application in high pressure processes such as reverse osmosis. On the other hand, the macrovoid structure is suitable for ultrafiltration processes and can be employed as support layers for composite membranes.[14]

Several mechanisms have been proposed to describe the formation of macrovoids. Matz[21] and Frommer and Lancet[22] suggested that the interfacial hydrodynamic instability driven by a surface tension gradient is responsible for the initiation of macrovoids. Strathman et al. proposed that precipitation rate determines macrovoid structure.[15] Ray et al. proposed that the formation of macrovoids is associated with the excess intermolecular potential gradients induced by the steep concentration gradient near the interface.[23] The study from Boom et al.[24] and Smolders et al.[14] also showed that macrovoid formation in phase separation occurs from freshly formed nuclei of the diluted phase when the composition in front of the nuclei remains stable for a relatively long period of time. Diffusion of solvent expelled from the surrounding polymer solution causes macrovoid growth. Macrovoids are generally formed in systems where instantaneous demixing takes place, except when the polymer additive concentration and the nonsolvent concentration in the polymer solution exceed a certain minimum value.[14,24−26] Therefore, the polymer solution composition close to the binodal composition favors the formation of spongy structures.

Cohen et al.[16] first calculated the diffusion path using the ternary phase diagram, which was later improved by many research groups to study membrane formation mechanisms.[17,18,27,28] According to the calculated diffusion path, instantaneous liquid−liquid demixing can account for the initiation of macrovoids quite well. It was also found that the miscibility between the solvent and the coagulant plays an important role in determining whether the membrane formation system demixes instantaneously.[17] The importance of the miscibility between the solvent and the coagulant was also noticed by Termonia[29] and Cheng et al.[30] For a more complete review of the formation mechanisms of macrovoids, one can refer to the works of Smolders et al.[14] and Paulsen et al.[31]

The slower nonsolvent uptake which occurs in vapor-induced phase separation (VIPS) favors solid−liquid demixing (polymer crystallization) over liquid−liquid demixing when this process is used to prepare membranes from a semicrystalline polymer like poly(vinylidene fluoride) (PVDF).[32] Li et al. have shown that PVDF membrane morphology can be controlled by adjusting polymer dissolution temperature.[33] Two gelling processes are occurring: crystallization-initiation and noncrystallization-initiation. Above a critical dissolution temperature, crystallization-initiation gelation outcompetes noncrystallization-initiation and forms nodular structures. Below this critical temperature, noncrystallization-initiation is the dominant gelling process and fibrillar structures are formed. The competition between the two gelling processes is vital in determining PVDF membrane morphology.

In summary, factors that affect the rate of liquid−liquid and solid−liquid demixing or polymer precipitation ultimately determine the physical morphology of membranes formed by nonsolvent induced phase separation. Membranes with these different physical morphologies finally have different separation properties and can be applied in various types of separation processes.

Table 2. Solvents for Cellulose Acetate and Polysulfone[3]

cellulose acetate	polysulfone
dimethylformamide (DMF)	dimethylformamide (DMF)
dimethylacetamide (DMAc)	dimethylacetamide (DMAc)
acetone	dimethylsulfoxide (DMSO)
dioxan	formylpiperidine (FP)
tetrahydrofuran (THF)	morpholine (MP)
acetic acid (HAc)	*N*-methylpyrrolidone (NMP)
dimethylsulfoxide (DMSO)	

3. INFLUENCE OF VARIOUS PARAMETERS ON MEMBRANE SEPARATION PERFORMANCE AND CHEMICAL PROPERTIES

3.1. Choice of Solvent. The choice of solvent−nonsolvent system in phase inversion membrane formation has a dramatic influence on membrane morphology, mechanical properties, interfacial characteristics, and separation performance. The polymer must be soluble or easily dispersible in the chosen solvent, and the solvent and nonsolvent must be miscible. There are usually several solvents that are compatible with a given polymer. For example, Table 2 lists several solvents that are compatible with cellulose acetate and polysulfone.[3]

There are a very large number of compatible solvent−nonsolvent pairs, each with their own specific thermodynamic behavior and miscibility. Frequently, the higher the mutual affinity (or miscibility) between the solvent and nonsolvent is, the more likely instantaneous demixing will occur and more porous membrane will be obtained.[3] In the case of low mutual affinity, an asymmetric membrane with a dense nonporous top layer is likely obtained. Although other parameters influence membrane structure, the choice of solvent−nonsolvent is crucial.[3]

Several approaches to determining polymer solubility have been developed. Flory and Huggins developed a two-dimensional lattice-based model to describe polymer solutions.[34−36] In this model, polymer segments and solvent molecules are assumed to be the same size, and only one molecule or polymer segment can occupy a single lattice site.[37] The Gibbs free energy of mixing, ΔG_m, is calculated as

$$\Delta G_m = kT(n_1 \ln \phi_1 + n_2 \ln \phi_2 + \chi_{12} n_1 \phi_2) \quad (23)$$

where k is Boltzmann's constant (1.38×10^{-23} J K^{-1}), T is absolute temperature, n_1 and n_2 are the number of solvent (component 1) and polymer (component 2) molecules, ϕ is the volume fraction, and χ_{12} is the Flory interaction parameter. The dimensionless Flory interaction parameter is a characterization of polymer−solvent interaction energy. Inverse gas chromatography is the most common method used to experimentally determine χ_{12}.[37,38] Modifications to the Flory−Huggins model have been made to describe dilute polymer solutions[39] and to account for the concentration dependence of χ_{12}.[40]

Solubility parameters, δ, may be used to estimate χ_{12} and help choose appropriate solvent−polymer matches. Solubility parameters of solvents are related to the molar energy of vaporization, ΔE^v, and molar volume, V, of a pure liquid by the following

$$\delta = \sqrt{\frac{\Delta E^v}{V}} \quad (24)$$

where ΔE^v represents the energy change after the isothermal vaporization of the saturated liquid to the ideal gas state at infinite dilution. The energy of vaporization is related to the enthalpy of vaporization by $\Delta E^V \approx \Delta H^V - RT$.[37]

The solubility parameters of polymers can be approximated from group contribution methods.[41−43] Polymer solubility parameters can also be determined experimentally by immersing polymer in different solvents whereby the polymer solubility parameter value is taken as that of the solvent which causes maximum polymer swelling.[37]

The Flory interaction parameter can be approximated from solvent (δ_1) and polymer (δ_2) solubility parameters using the following relation:

$$\chi_{12} = \frac{v_1}{RT}(\delta_1 - \delta_2)^2 \quad (25)$$

where v_1 is the molar volume of the solvent and R is the ideal gas constant.[37] Scatchard and Hildebrand estimated the heat of mixing, ΔH_m, using polymer and solvent solubility parameters by the following relation:

$$\Delta H_m = V_m(\delta_1 - \delta_2)^2 \phi_1 \phi_2 \quad (26)$$

where V_m is the molar volume of the mixture.[44,45] Solvents can be matched to polymers by using the Scatchard−Hildebrand equation to minimize the heat of mixing. However, this equation is only applicable for $\Delta H_m > 0$ and does not account for specific interactions such as hydrogen bonding.

Hansen proposed that the total energy of vaporization of a liquid was due to dispersion forces, permanent dipole−permanent dipole forces, and hydrogen bonding.[46−51] Therefore, the solubility parameter, which is related to the total cohesive energy, should be broken into three components: dispersive (δ_d), polar (δ_p), and hydrogen bonding (δ_h). The total, or Hildebrand, solubility parameter is equal to

$$\delta = \sqrt{\delta_d^2 + \delta_p^2 + \delta_h^2} \quad (27)$$

Calculation of solvent δ_d and δ_p is described by Blanks and Prausnitz.[52] Hansen and Beerbower found that solvent δ_p could be calculated as

$$\delta_p = 37.4 \frac{\mu}{V^{0.5}} \quad (28)$$

where μ is the solvent dipole moment and V is the solvent molar volume.[48] Solvent hydrogen bonding solubility parameter has typically been calculated by subtracting δ_d and δ_p from δ. The group contribution method is also a viable approach to calculating δ_h. Hansen believes the group contribution approach is best for determining solubility parameters for polymers.[53] A solubility parameter distance, Ra, was developed by Skaarup.[51] This "distance" between polymer (1) and solvent (2) is a measure of their affinities based on their individual Hansen solubility parameters, which is calculated below as

$$Ra = \sqrt{4(\delta_{d2} - \delta_{d1})^2 + (\delta_{p2} - \delta_{p1})^2 + (\delta_{h2} - \delta_{h1})^2} \quad (29)$$

The relative energy difference, RED, is equal to Ra/R_o, where R_o is the radius of interaction of a Hansen solubility parameter sphere. The RED should not exceed a value of 1 if solubility is to be maintained. Solubility increases as RED approaches 0. The radii of interaction (R_o) for several common polymers are tabulated by Hansen.[54] Sample RED values are tabulated below for cellulose acetate and polysulfone (Table 3a and 3b).[54] Several potentially compatible solvents (RED < 1) can be quickly and easily selected using this model and published solubility parameters.

Table 3a. Relative Energy Density Calculation for Several Common Solvents and Cellulose Acetate[53]

	δ_d (MPa$^{1/2}$)	δ_p (MPa$^{1/2}$)	δ_h (MPa$^{1/2}$)	Ro (MPa$^{1/2}$)	
cellulose acetate	16.9	16.3	3.7	13.7	
	δ_d (MPa$^{1/2}$)	δ_p (MPa$^{1/2}$)	δ_h (MPa$^{1/2}$)	Ra (MPa$^{1/2}$)	RED
acetic acid	14.5	8	13.5	13.7	1.0
acetone	15.5	10.4	6.9	7.3	0.5
acetonitrile	15.3	17.9	6.1	4.3	0.3
benzene	18.4	1	2.9	15.6	1.1
n -butanol	15.9	5.7	15.7	16.1	1.2
butyl acetate	15.8	3.7	6.3	13.1	1.0
carbon tetrachloride	17.6	0	0	16.8	1.2
chloroform	17.6	3	4.2	13.4	1.0
cyclohexane	16.7	0	0	16.7	1.2
1,2-dichloroethane	19	7.4	4.1	9.8	0.7
dichloromethane	18.2	6.3	7.8	11.1	0.8
N,*N*-dimethylacetamide	16.8	11.5	10.2	8.1	0.6
dimethylformamide	17.4	13.7	11.2	8.0	0.6
dimethyl sulfoxide	18.4	16.3	10.2	7.2	0.5
dioxane	16.8	5.7	8	11.4	0.8
ethanol	15.8	8.8	19.4	17.5	1.3
ethyl acetate	15.8	5.3	7.2	11.8	0.9
diethyl ether	19	1.8	7.4	15.5	1.1
heptane	15.1	0	0	17.1	1.2
hexane	14.8	0	0	17.2	1.3
methanol	15.1	12.2	22.2	19.3	1.4
methyl-*t*-butyl-ether	15.5	3.6	5.2	13.1	1.0
methyl ethyl ketone	15.9	9	5.1	7.7	0.6
N-methyl-2- pyrrolidone	18	12.3	7.2	5.8	0.4
pentane	14.3	0	0	17.5	1.3
n-propanol	15.8	6.7	17.3	16.8	1.2
isopropanol	15.8	6.1	16.4	16.4	1.2
di-isopropyl ether	14.4	2.9	5.1	14.4	1.0
tetrahydrofuran	19	10.2	3.7	7.4	0.5
toluene	18	1.4	2	15.2	1.1
trichloroethylene	18	3.1	5.3	13.5	1.0
water	15.5	16	42.3	38.7	2.8
xylene	17.6	1	3.1	15.4	1.1

3.2. Choice of Polymer. For porous membranes, the type of polymer will affect solute adsorption, membrane hydrophilicity, and the thermal and chemical stability of the membrane. For nonporous membranes, the choice of polymer directly affects membrane performance because intrinsic membrane separation properties (solubility and diffusivity) depend on polymer chemical structure, and, hence, on the choice of polymer. In nonsolvent induced phase separation, the choice of polymer is an important factor because it limits the solvents and nonsolvents that can be used in the phase inversion process. In addition, the solvent also plays an important role along with polymer concentration during membrane formation.

Many different polymers are used in the synthesis of microfiltration, ultrafiltration, nanofiltration, and reverse osmosis membranes. Polysulfone (PSf), polyethersulfone (PES), polyacrylonitrile (PAN), cellulosics, poly(vinylidene fluoride) (PVDF), poly(tetrafluoroethylene) (PTFE), polyimides (PI), and polyamides (PA) are among the most common polymeric membrane materials in use today. Each of these polymers is briefly discussed in the following.

3.2.1. Polysulfone. Polysulfone (PSf) is one of the most common polymers used to make membranes by phase inversion process. Polysulfone is often selected because of its commercial availability, ease of processing, favorable selectivity-permeability characteristics, and glass transition temperature (T_g) value of 190 °C. It possesses good mechanical, thermal, and chemical properties. Moreover, it is generally easy to prepare asymmetric membranes by the phase inversion method, in which a thin layer of PSf solution in an appropriate solvent is immersed into the nonsolvent coagulation bath, such as water. The solvents most frequently used for PSf are *N*-methylpyrrolidone (NMP),[55−63] *N*,*N*-dimethylacetamide (DMAc),[58,59,61,64,65] and *N*,*N*-dimethylformamide (DMF).[66,67]

3.2.2. Polyethersulfone. Polyethersulfone (PES) possesses very good chemical and thermal stability as indicated by its glass transition temperature (T_g) value of 230 °C. This polymer is also widely used as support material for composite membranes. Like polysulfone, it is generally easy to prepare asymmetric membranes with water as a coagulant by the phase inversion method. The solvents usually used for PES are *N*-methylpyrrolidone (NMP),[68−73] *N*,*N*-dimethylformamide (DMF),[67,69,74] and *N*,*N*-dimethylacetamide (DMAc).[73,75−77]

3.2.3. Polyacrylonitrile. Polyacrylonitrile (PAN) is also a popular membrane material because it is a resinous, fibrous, or rubbery organic polymer with sufficient chemical stability and hydrophilicity. Other common membrane materials such as PSf and PES are relatively hydrophobic and prone to fouling whereas PAN membranes are relatively hydrophilic, low fouling in aqueous filtration applications, and are already commercialized.[78] Polyacrylonitrile has good resistance to solvents and cleaning agents such as chlorine and sodium hypochlorite. Polyacrylonitrile has been used as a substrate for MF, UF, NF, RO, and pervaporation membranes.[79−85] It is very difficult to reduce the pore size of PAN membranes due to its poor solubility in various solvents except polar solvents such as NMP,[81,86] DMF,[87−89] and DMAc.[89−91]

3.2.4. Cellulosics. Cellulosics generally include cellulose acetate, cellulose acetate butyrate, and cellulose propionate, all of which are cellulose esters. Cellulose acetate was the first cellulosic polymer used to form phase inversion membranes[21,92] and is the most frequently employed to prepare membranes.[93−96] Cellulose acetate has low chemical, mechanical, and thermal resistance. Cellulosics can be used in ultrafiltration applications or be made into RO membranes by nonsolvent induced phase separation. Cellulose acetate can be made into a film or into a fiber, but it must be chemically modified to produce a thermoplastic material. It is mainly used as a material for dialysis membranes. Cellulose acetate is frequently blended with other polymers such as PSf or additives such as polyethylene glycol (PEG) to improve the membrane properties.[93,96−99] Cellulose triacetate can be used to form chlorine tolerant hollow fiber RO membranes.[100,101]

3.2.5. Polyimides (PI)/Polyamides (PA). Polyimides are a group of polymers with good gas selectivity and chemical stability, and excellent thermal stability. Therefore, in recent years studies have been performed for their application as membrane materials.[102−105] Polyamide membranes are mechanically very strong and exhibit excellent wet and dry strength.[106] Their hydrophilicity makes them suitable for aqueous and organic solutions.[107,108] *N*-methylpyrrolidone (NMP) is most widely used as a solvent for these two polymers.[102,103,105]

Table 3b. Relative Energy Density Calculation for Several Common Solvents and Polysulfone[53]

	δ_d (MPa$^{1/2}$)	δ_p (MPa$^{1/2}$)	δ_h (MPa$^{1/2}$)	Ro (MPa$^{1/2}$)	
polysulfone	19.7	8.3	8.3	8.0	
	δ_d (MPa$^{1/2}$)	δ_p (MPa$^{1/2}$)	δ_h (MPa$^{1/2}$)	Ra (MPa$^{1/2}$)	RED
acetic acid	14.5	8	13.5	11.6	1.5
acetone	15.5	10.4	6.9	8.8	1.1
acetonitrile	15.3	17.9	6.1	13.2	1.7
benzene	18.4	1	2.9	9.4	1.2
n-butanol	15.9	5.7	15.7	10.9	1.4
butyl acetate	15.8	3.7	6.3	9.3	1.2
carbon tetrachloride	17.6	0	0	12.5	1.6
chloroform	17.6	3	4.2	7.9	1.0
cyclohexane	16.7	0	0	13.2	1.6
1,2-dichloroethane	19	7.4	4.1	4.5	0.6
dichloromethane	18.2	6.3	7.8	3.6	0.5
N, N-dimethylacetamide	16.8	11.5	10.2	6.9	0.9
dimethylformamide	17.4	13.7	11.2	7.7	1.0
dimethyl sulfoxide	18.4	16.3	10.2	8.6	1.1
dioxane	16.8	5.7	8	6.4	0.8
ethanol	15.8	8.8	19.4	13.6	1.7
ethyl acetate	15.8	5.3	7.2	8.4	1.1
diethyl ether	19	1.8	7.4	6.7	0.8
heptane	15.1	0	0	14.9	1.9
hexane	14.8	0	0	15.3	1.9
methanol	15.1	12.2	22.2	17.1	2.1
methyl-*t*-butyl-ether	15.5	3.6	5.2	10.1	1.3
methyl ethyl ketone	15.9	9	5.1	8.3	1.0
N-methyl- 2- pyrrolidone	18	12.3	7.2	5.4	0.7
pentane	14.3	0	0	16.0	2.0
n-propanol	15.8	6.7	17.3	12.0	1.5
isopropanol	15.8	6.1	16.4	11.5	1.4
di-isopropyl ether	14.4	2.9	5.1	12.3	1.5
tetrahydrofuran	19	10.2	3.7	5.2	0.6
toluene	18	1.4	2	9.9	1.2
trichloroethylene	18	3.1	5.3	6.9	0.9
water	15.5	16	42.3	35.9	4.5
xylene	17.6	1	3.1	9.9	1.2

3.2.6. Fluoropolymers. Fluoropolymers frequently used to prepare membranes include polytetrafluoroethylene (PTFE) and poly(vinylidene fluoride) (PVDF). Both polymers are hydrophobic and exhibit good chemical and thermal stability due to their chemical structure. Their hydrophobic nature makes them useful materials in membrane distillation.[3] Microfiltration membranes formed from PTFE may be prepared by sintering and stretching whereas PVDF membranes are made by phase inversion.[3,109−115] Poly(vinylidene fluoride) shows good thermal and chemical resistance, although not quite as good as PTFE. Poly(vinylidene fluoride) is soluble in aprotic solvents such as DMF, DMAc, NMP, and triethylphosphate (TEP).

3.3. Polymer Concentration. Polymer concentration in the dope solution is yet another parameter affecting membrane morphology. Typical polymer concentration ranges from 15 to 25 wt %.[116] Increased polymer concentration in the casting solution results in higher polymer concentration at the nonsolvent interface.[71] This implies that the volume fraction of polymer increases and consequently a lower porosity is obtained. When polymer concentration is increased beyond a certain value, the resulting membrane has lower porosity and the pure water flux can be reduced to zero despite the occurrence of instantaneous demixing. Strathmann et al.[12,15] focused on the effect of polymer concentration on membrane morphology. Their research demonstrated that varying initial polymer solution concentration changes the path to precipitation, which can be shown from the ternary phase diagram. Two different structures were obtained depending on the different ways of precipitation.

3.4. Choice and Composition of Nonsolvent System. The choice of nonsolvent will influence the precipitation. When a polymer solution is cast as a thin film upon a support and then immersed in the nonsolvent, the miscibility of solvent and nonsolvent and the affinity between polymer and nonsolvent will affect the demixing rate and finally influence the final membrane structure.[3] Water is frequently used as a nonsolvent, but other nonsolvents such as acetone and lower aliphatic alcohols are also used.[117−120] The addition of solvent to the coagulation bath is another parameter that influences the membrane structure. However, the maximum amount of solvent that can be added is determined by the position of the binodal of the phase diagram. By adding solvent to the coagulation bath, instantaneous demixing can be stopped. A delay in demixing occurs, which leads to the formation of a nonporous membrane. This effect is unusual because there appears to be two competing processes. The addition of solvent to the coagulation bath lowers the polymer concentration at the film interface. This would lead to a more open membrane.[3,121] Addition of solvent to the coagulation bath lowers the nonsolvent activity and diffusion rate into the polymer film, which further delays demixing. Ghosh et al. found that by adding a small percentage of solvent to the coagulation bath (3% NMP in water) membrane permeability could be increased by more than 25%.[11] Others believe that the delay in liquid−liquid demixing is the dominant effect as this method is typically used to produce dense films.[3] In addition, other additives to the coagulation bath such as methanol, isopropanol, and salt were found to affect the demixing process.[9,89,117,122]

3.5. Additives to the Polymer Solution. A number of researchers have studied the role of additives on membrane structure. Most casting solutions contain high or low molecular weight additives for improving the morphology and function of phase inversion membranes, which makes analysis of solvent−nonsolvent system properties more complex. The addition of organic or inorganic components as a third component to a casting solution has been one of the important techniques used in membrane preparation. The addition of these additives can create a spongy membrane structure by preventing finger-like macrovoid formation, enhance pore formation, improve pore interconnectivity, and increase hydrophilicity. For example, finger-like macrovoid formation can be suppressed by the addition of polyvinylpyrrolidone (PVP). Other frequently used additives include polyethylene glycol (PEG), propionic acid (PA), surfactants such as sorbitan monoleate (Span-80), alcohols, dialcohols, water, polyethylene oxide (PEO), LiCl, and $ZnCl_2$. Here, the general results of adding PVP, PA, PEG, and surfactant will be discussed.

3.5.1. Polyvinylpyrrolidone. Boom et al.[24,123] studied the role of polyvinylpyrrolidone (PVP) as a polymeric additive in the

formation of polyethersulfone (PES)/NMP membranes. They found the addition of PVP suppresses the formation of macrovoids. Polyvinylpyrrolidone can become entrapped in polymeric films and impart some hydrophilic character.[124] This hydrophilic additive may also leach out of membranes after many hours of operation.[125] Several studies have since been reported on PVP additives of varying molecular weight[58,103,111,126,127] and concentration[57,71,76,96,98,128−130] in an attempt to improve membrane morphology and function.

Yeo et al. concluded that PVP addition to the casting solution of PSf and DMF contributed to the enlargement of the macrovoid structure in the prepared membranes rather than the suppression of that structure.[131] This was confirmed by Jimenez et al. through molecular weight cut off (MWCO) and pure water permeation tests.[71]

The study of Yoo et al. explained that adding PVP of different molecular weights into casting solutions produced membranes with significantly different morphologies.[103] Addition of 40 kDa PVP increased macrovoid formation. However, addition of 360 kDa PVP suppressed the formation of finger-like macrovoids. The authors suggest that changes in solution viscosity brought on by addition of PVP alter the rate of phase separation, which ultimately causes the differences in membrane morphology. Chakrabarty et al. also studied an increase from 24 to 360 kDa PVP added to the casting solution.[58] As PVP molecular weight increased, membrane sublayers had dense structures with fewer macrovoids, and the pore number and porosity of the prepared membrane was found to increase. Membrane skin layers were found to be thicker as more PVP was added, and the number of finger-like macrovoids gradually disappeared. Jung et al. concluded that the top layers became thicker as more PVP was added, and the number of finger-like macrovoids gradually disappeared in the membrane. Hypochlorite was successfully used to wash out residual PVP[127]

3.5.2. Polyethylene Glycol. Polyethylene glycol (PEG) is also frequently added to the casting solution as a third component in membrane preparation. Studies have investigated the effect of PEG additives with different molecular weights.[59−61,70,74,97,98,109,132,133] Polyethylene glycol acts as a pore-forming agent and also affects the thermodynamics and kinetics of the phase inversion process. Kim et al. systematically studied the effect of PEG on membrane formation by phase inversion.[60] The study showed that by increasing the ratio of PEG additive to solvent NMP, the casting solution becomes thermodynamically less stable. Membrane surface pore size becomes larger, and the top layer becomes more porous. Shieh et al. extended that PEG, being hydrophilic in nature, can be used to improve membrane selectivity and as a pore-forming agent.[134] Kim and Lee investigated the effect of various PEG molecular weights on the formation of polyetherimide (PEI) asymmetric membranes.[133] They reported that small molecular weights of PEG, such as PEG 200, work as a pore-reducing agent for PEI membranes. Zheng et al. found that PEG addition could thermodynamically enhance and rheologically hinder PSf solution demixing.[61] Also, their research compared the cross-sectional morphologies of membranes prepared at different coagulation bath temperatures.[64] When PSf concentration is 18 wt % and the coagulation bath temperature is 20 °C, the size of finger-like macrovoids increases and then decreases rapidly with increasing PEG concentration.

The effects of PEG concentration have also been studied in other solvent systems. The research of Liu et al. showed that PEG can be used to enhance polymer (PES) solution viscosity and to enhance pore interconnectivity when added in appropriate amounts.[70] The effects of PEG on the porosity of polycarbonate (PC) membranes prepared via dry-/wet-phase inversion methods was studied by Deniz.[135] It was observed that membrane porosity increased with an increase in the initial PEG concentration ranging from 5 to 20 wt %. Idris et al.[74] and Chakrabarty et al.[59] reported the effect of PEG with different molecular weights from 400 to 20 000 Da on morphology and performance of PSf membranes. They showed that PEG 6000 can be a suitable additive for making asymmetric membranes having a dense skin layer and a relatively macrovoid-free sponge-type support layer. By increasing the molecular weight of PEG, the pore number and porosity of the prepared membrane was increased, so PEG can be regarded as a pore-forming agent rather than a pore-reducing agent in this case.

3.5.3. Propionic Acid. Propionic acid has been studied as an additive by many research groups. Fritzsche et al. reported that when a PSf solution film is rapidly formed by immersion precipitation, the propionic acid added in the casting solution increased the gas permeability by nearly 10-fold.[136] Han showed that by adding propionic acid to the coagulation bath, polymer packing density significantly decreased in membranes made by phase inversion.[63] The decrease is due to both the significant increase of nodule structures and the pore formation between polymer aggregates. Laninovic showed that the addition of propionic acid in a polymer solution inhibited the growth of macrovoids, which resulted in improved mechanical characteristics of the formed membranes.[137] Water fluxes through the membranes prepared from a polymer solution with propionic acid had a lower value in relation to a membrane prepared from a polymer solution without an additive.

3.5.4. Surfactants. The addition of surfactants can affect the membrane structure because it can dramatically affect the interfacial properties between the coagulant and the polymer solution. The study by Lin et al. proposed that the addition of appropriate surfactants can enhance the affinity between solvent and coagulant, resulting in a shift from delayed demixing to instantaneous demixing, and macrovoids can then be induced.[138] Later they extended the study to a dual-bath system, in which casting solution was immersed in one coagulant for a very short time (<2 s) and then moved to a second bath containing different coagulants. They found that the difference in the void structure can be explained by the difference in the growth mechanism of macrovoids. For the system polymethylmethacrylate (PMMA)/NMP/water, the growth of macrovoids is by convection. For the system PMMA/acetone/Tween80/water, the growth of macrovoids is by diffusion.[139,140] Tsai et al. systematically studied the effect of sorbitan monooleate series surfactant as an additive on the structure of polysulfone membranes.[55,56,141,142] From their research, addition of surfactant (Span-80) in the casting solution can suppress macrovoids in asymmetric PSf membranes. Also, they studied the effects on membrane structure using Span-20 and Span-80 at different concentrations.[56] The results showed that the addition of Span-80 could effectively inhibit the formation of vast macrovoids, and penetration experiments offered a reasonable explanation for this observation, suggesting that macrovoid formation was inhibited by the reduction of the water penetration rate.

3.5.5. Other Chemicals. Besides PVP, PA, PEG, and surfactants, some other small molecules can be used as additives. Kim et al. tried acetic acid (AA) as an additive to the system of

polyetherimide/NMP/water.[143] They showed that increasing the content of AA makes the membrane cross-section a closely connected, cellular sponge-type structure. Acetone has been used as an additive in PSf/DMF/water, PES/DMF/water, and PSf/NMP/water systems to compare the finger-like pores formed by PES and PSf.[67,144] Butanol, propanol, and chloroform have also been applied as polar and nonpolar additives to show that the polar additive caused rapid demixing and formed porous asymmetric membranes with defective skin layers. The nonpolar additive decreases the demixing rate of the casting solution in this ternary system.[144]

3.5.6. Nanoparticles as Additives. Inorganic particles have been used as fillers in various applications ranging from clothing to tennis racquets and computer circuits to improve properties such as stiffness, toughness, chemical stability, electrical conductivity, and resistance.[145] Typically used fillers are on the order of nanometers and because of their size are needed at concentrations as high as 20% by volume, which limits their application.[146] Therefore, a composite with improved properties and lower particle concentration is sought after. Nanocomposites are one possible solution.

When all three dimensions of a particle are on the order of nanometers, such as a spherical particle, it is referred to as an isodimensional nanoparticle.[147−149] If only two dimensions are in the nanometer range, an elongated structure is formed and the structure formed is referred to as a nanotube, nanofiber, or whisker.[150−152] Particles with only one nanoscale dimension form flat sheets. These three categories are used in different applications.

The use of nanoparticles as a filler in polymeric membranes, creating polymer nanocomposites, has begun to attract wide interest due to the improved electrical and mechanical properties, such as increased strength and modulus.[37] The improved properties result from a microstructure with a large fraction of filler atoms at the surface of the nanoparticles and the strong interfacial interactions the nanoparticles have with the surrounding polymer.[146] Isodimensional nanoparticles are typically used because they provide the best surface area to volume ratio. Nanoparticles based on materials such as clays, zeolites, carbon nanotubes, metals, and oxides have been explored in polymeric membranes, but the use of nanoparticles in formation of thin film composite membranes for desalination is an emerging area of research.[153,154]

3.6. Formation Temperature. Temperature is a parameter that affects the viscosity of the casting solution. Casting solution viscosity can affect the exchange rate of solvent and nonsolvent during phase inversion. Therefore, temperature can be considered an influential parameter on membrane formation kinetics and surface and internal membrane morphology.[55,60,89,129,155,156] Because a cloud-point curve represents an approximate boundary when liquid−liquid demixing occurs, it should be a good method to depict the thermodynamic process of phase inversion.

The research of Tsai et al. showed that coagulation bath temperature had tremendous influence after adding surfactants to polysulfone casting solution.[55] They found that temperature affects the viscosity of the coagulation bath and finally the size of the formed macrovoids. Zheng et al. studied the influence of temperature on the viscosity of the casting solution.[61] They showed that increasing casting solution temperature decreased polysulfone casting solution viscosity and increased solvent−nonsolvent miscibility. They also showed that with the increase of temperature, the kinetic parameter of membrane formation, D_a, ($= d^2/t$, where d is membrane thickness and t is coagulation time) increased. Zheng et al. also measured the cross-sectional morphologies of membranes prepared at different coagulation bath temperatures.[64] The size of finger-like macrovoids increased with increased coagulation bath temperature.

4. CHARACTERIZATION OF PHASE INVERSION MEMBRANES

The performance, stability, and durability of a membrane are determined largely by their chemical composition and physical morphology. These properties can be characterized by a wide range of analytical methods. Understanding the fundamental characteristics of the membrane not only help to select a proper membrane for specific applications, but also guide the design of membranes with desired properties.[157] This section is by no means an exhaustive effort in accounting for all characterization methods; rather, it provides general fundamental principles and knowledge of membrane characterization techniques to obtain the essential information correlating membrane properties with their performance.

4.1. Kinetics and Thermodynamics of Membrane Formation. *4.1.1. Process Kinetics.* The solvent−nonsolvent exchange rate is one of the kinetic factors attracting the most attention. It determines the path on the phase diagram during membrane formation. The method used for kinetic characterization is to observe the penetration of nonsolvent into the casting solution. This technique was described in the research of Frommer and Lancet,[22] Strathmann et al.,[15] and Wang et al.[158] In their methods, they placed a drop of the casting solution between two microscope slides and a drop of the coagulant (distilled water), added with phenolphthalein or rhodamine B in order to better observe the movement in precipitation. The coagulant penetrated into the casting solution when they were brought into contact. The penetration fronts of water and rhodamine B into the casting solutions were observed and videoed with an optical microscope. The video then was analyzed by image processing software to determine the time dependence of the water penetration, from which the demixing rate of the chosen solvent−nonsolvent system can be measured. This demixing rate finally determines the structure of the membrane as mentioned in a previous section.

4.1.2. System Thermodynamics. System thermodynamics are generally demonstrated by a ternary phase diagram. The binodal curve of liquid−liquid phase separation was considered an important factor affecting the membrane structure. Cloud points are defined as the moment when the solution changes from clear to turbid. The cloud point curve was usually measured to represent the binodal curve. To determine the composition or temperature at which the solution is no longer thermodynamically stable, turbidity or cloud points must be determined.[3]

For the construction of binodal curves, the titration method is described[159] and widely used.[15,56,160] In this case, the nonsolvent or a mixture of the solvent and nonsolvent is added slowly to a solution of the polymer and solvent. During titration, the polymer solution is well stirred and kept at a constant temperature. The composition at which permanent turbidity occurs is the cloud point, which represents the composition where phase transition occurs. This technique can be operated visually. When the mixing solution changes from clear to turbid, the volume of

the solvent solution and the volume of the nonsolvent solution are recorded, and the exact cloud point is determined.

Another technique is cooling. With this technique, a tube is filled with either a binary mixture of polymer/solvent or a ternary mixture of polymer/solvent/nonsolvent and then sealed. The solution is homogenized at elevated temperature and the temperature of the thermostat bath is then decreased slowly at a constant cooling rate. At a certain temperature the solution is no longer thermodynamically stable and demixing occurs, which causes the solution to become turbid. This technique can be operated visually or by light transmission. The cloud point is observed when the reading of the light transmission instrument increases sharply.[3]

4.2. Membrane Physical and Chemical Properties. *4.2.1. Membrane Thickness.* For membranes prepared by the way of nonsolvent induced phase inversion, the thickness of the sublayer is usually between 50 and 200 μm, while the skin layer is a few micrometers or less. A micrometer is widely used to measure the total thickness of a porous filtration membrane. For approximation of skin layer thickness, generally scanning electron microscopy (SEM) is used, which can provide a clear view of the overall structure of the membrane, the skin layer, and the cross-section.[69,161]

4.2.2. Membrane Porosity and Pore Size Distribution. Much effort has been made to characterize the pore size, pore size distribution, and solute or particle rejection for filtration membranes. Methods to characterize membranes can be classified into (1) physical methods to determine pore size and pore size distribution of a membrane and (2) methods based on permeation and rejection performance using reference molecules and particles.[162]

4.2.2.1. Physical Methods. For characterizing the pore size and pore size distribution from rejection data, quantitative transport models, such as the Hagen−Poiseuille equation, were used. Nakao[162] and Zhao et al.[163] have given reviews for determination of membrane pore size and pore size distribution. The following physical methods for pore size and pore size distribution determination are well-known: (1) microscopic, (2) bubble pressure and gas transport, (3) mercury porosimetry, (4) liquid−vapor equilibrium, (5) liquid−solid equilibrium (thermoporometry), and (6) gas−liquid equilibrium (permporometry).

Electron microscopy (EM) is one of the most powerful tools that can provide detailed information about the pore size, pore shape, morphology, and structure of membranes. Scanning electron microscopy (SEM) and transmission electron microscopy (TEM) are the two most commonly used EM methods. The operational principle of SEM relies on the detection of different scattered electrons by scanning the sample surface with a high energy electron beam. To observe cross sections by SEM the dried membrane is first fractured at liquid nitrogen temperature, and then fixed perpendicularly to the sample holder. Pores larger than 1 nm can be imaged by SEM.[58,59,89] In contrast, TEM measurement analyzes the transmitted or forward-scattered electrons through the specimen.[164] The dried sample is first embedded and then sliced by a microtome. An embedding media with no influence on the membrane must be chosen. Both SEM and TEM are more widely used in recent years because of their convenient operation.[162,165−167]

The bubble point method was used in the early years of the last century. This method essentially measures the pressure needed to blow air through a liquid-filled membrane. As the air pressure is gradually increased, bubbles of air penetrate through the membranes at a certain pressure. It is a simple technique for characterization of the largest pores in microfiltration membranes. However, different results will be obtained when different liquids are chosen, and the rate of pressure increase and the pore length may influence the result.[162] If water is used as the wetting medium, then this method can measure pores down to a few nanometers.[3]

The mercury intrusion technique is a variation of the bubble-point method. In this technique, mercury wets the membrane and is forced into a dry membrane with the volume of the mercury being determined at each pressure. The relationship between pressure and pore size is given by the Laplace equation. All microfiltration membranes, as well as a substantial proportion of ultrafiltration membranes, can be characterized using this method (pore size from 5 nm to 10 μm). The disadvantage is that the apparatus is rather expensive and some small pore sizes require high pressure, which may damage membrane structure.[3,168]

The liquid−vapor equilibrium method was employed in the past.[169] This method for calculating pore size distributions is based on a model of the adsorbent as a collection of cylindrical pores. The theory accounts for capillary condensation in the pores using the classical Kelvin equation, which in turn assumes a hemispherical liquid−vapor meniscus and a well-defined surface tension. This theory also incorporates thinning of the adsorbed layer through the use of a reference isotherm.

Introduced by Brun et al., thermoporometry is based on the calorimetry of a solid−liquid transition in a porous material.[170] The principle is that the temperature at which the water in the pores freezes depends on the pore size. As the pore size decreases the freezing point of water decreases. So through the measurement of the freezing point, the pore size can be obtained. It is a simple method but all pores are measured with this technique, including dead-end pores, which make no contribution toward transport.[170−172]

Permporometry is based on the blockage of pores with a condensable gas while simultaneously measuring gas flux through the membrane. This technique can only characterize the active pores which contribute to the transport. However, this technique is difficult to employ especially for hollow fiber membranes due to the difficulty of maintaining the same pressure on both sides of the membrane.[167,173]

4.2.2.2. Permeability and Rejection Test. Methods based on permeation and rejection performance can also be employed to determine the pore size and pore size distribution of membranes.[3] The pore size can be obtained by measuring the flux through a membrane at a constant pressure using the Hagen−Poiseuille equation,

$$J_v = \frac{\varepsilon {r_p}^2}{8\mu\tau}\frac{\Delta p}{\Delta x} \tag{30}$$

Here J_v is the water flux through the membrane at a driving force of $\Delta p/\Delta x$, with Δp being the pressure difference across the membrane of thickness Δx. The proportionality factor contains the pore radius r_p, liquid dynamic viscosity μ, surface porosity of the membrane ε, and the tortuosity factor τ. The pore size distribution can be obtained by varying the pressure, i.e., by a combination of the bubble-point method and permeability methods. It is not essential that the liquid should wet the membrane. The permeability method is widely employed both

for microfiltration and ultrafiltration membranes because it has the distinct advantage of experimental simplicity, especially when liquids are used. However, the Hagen−Poiseuille equation assumes that pores are cylindrical, so the geometry is very important and will affect the result. For asymmetric membranes, Δx is the skin layer thickness and must be known to determine pore size.

The pore size of a filtration membrane can be described by the membrane's ability to retain solutes or particles of a given size or molecular weight. The term *molecular weight cutoff* is used to relate the size of a solute that would be retained, or almost completely retained, by a given membrane to that membrane's pore size.[2] Molecular weight cutoff is determined by performing rejection tests using solutes or globular proteins of known sizes with the membrane of interest. Figure 5 shows the comparison between a membrane with a so-called "sharp cutoff" and a membrane with a "diffuse cutoff". Solutes used in molecular weight cutoff tests should ideally be soluble in water or in a mildly buffered solution, cover a wide range of sizes, and should not adsorb to the membrane surface. Average pore size and pore size distribution can be determined from solute rejection data.[162]

Solute rejection measurements provide a very simple technique for determining membrane performance. However, some other factors such as adsorption, concentration polarization, and membrane fouling can have a drastic effect on the result, so it is difficult to obtain quantitative results by such a method.

4.2.3. Membrane Interfacial Properties. Composite membrane properties are determined largely by the extremely thin skin layer, so surface characterization is necessary. A wide range of physical and chemical surface analysis techniques are available. Here, some popular analytical methods are briefly summarized in Table 4.[174] In many situations, several connected processes may be going on more or less simultaneously, with a particular analytical technique picking out only one aspect (e.g., the extent of incident light absorption or the kinetic energy distribution of ejected electrons).

4.2.3.1. Surface Morphology. The surface morphology of membranes can also be examined by atomic force microscopy (AFM). The working principle of AFM is to use a sharp tip to scan the sample surface. When the tip is close to the surface, van der Waals forces will change the vibrating frequency of the tip or cause deflections. By detecting the vibrating frequency or deflections of the tip, a three-dimensional map of membrane surface topography can be obtained. Atomic force microscopy is widely used to characterize membrane surfaces and has the advantage of providing quantitative nanoscale measurements of both lateral and vertical morphology. In addition to morphology mapping, AFM can quantify the interaction force between the membrane surface and the probe used. Thus, much information besides the surface morphology, such as the fouling propensity and electrical properties, can be revealed.[175,176]

4.2.3.2. Membrane Chemical Structure. Many methods used to analyze chemical compounds can also be used to obtain the same information for membranes. The analytical methods generally used to examine the chemical composition of membranes include Fourier transform infrared spectroscopy (FTIR), Raman spectroscopy, energy-dispersive X-ray spectroscopy (EDX), electron spectroscopy for chemical analysis (X-ray photoelectron spectroscopy) (ESCA, XPS), auger electron spectroscopy (AES), electron energy loss spectroscopy (EELS), atomic force microscopy (AFM), and secondary ion mass spectrometry (SIMS). It should be noted that each analytical method has its unique operation principles, and the information obtained differs. Thus, combining several methods is generally required to infer the correct chemical composition of an unknown or novel membrane. The operation principles and applicability of some popular analytical methods will be discussed in the following section. Table 4 briefly summarizes the general information of applicability of some popular analytical methods.[174]

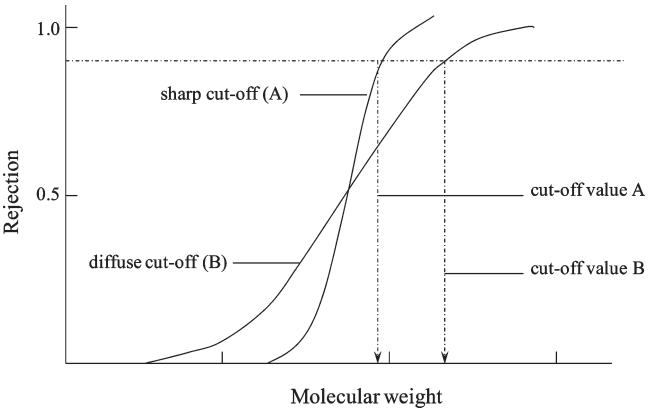

Figure 5. Rejection characteristics for a membrane with (A) a "sharp cut-off" compared with that of a membrane with (B) a "diffuse cut off".[3]

In general, XPS, AES, SIMS, EELS, and EDX are most suitable to obtain chemical information for membrane skin layers due to their low penetration capability. In contrast, Raman and FTIR reveal the chemical composition of both surface layer and the bulk materials. Another great advantage of Raman, FTIR, and AFM is the possibility of analyzing samples in their wet state, which is more relevant to membrane applications. If considering the lateral resolution in mapping the chemical composition of membranes, EDX, XPS, and AFM give more detailed information on the surface composition than other methods.[157]

Fourier transform infrared spectroscopy and Raman are two nondestructive methods commonly used to probe the lateral and vertical chemical composition of membranes. Both methods allow identification of the molecular bonds existing in the membrane and subsequently determination of the chemical structure. Besides providing the overall chemical composition, recent development in FTIR and Raman spectrometry has enabled depth profiling of the membrane surface.[177,178] By tuning the incident angle, the refractive indices of crystals, and the wavelength, the penetration of the IR signal into the membrane sample can be controlled. Thus, FTIR is suitable to reveal vertical chemical information of membrane samples with a spatial resolution of 0.5 to 1 μm.[157]

The surface chemical composition of membranes can also be revealed by EDX/EDS, XPS, and SIMS qualitatively and quantitatively. The operational principle of EDX/EDS relies on the detection of characteristic X-ray emitted from the specimen surface induced by incident of high energy beam. As each element has a unique energy of X-ray emission, the elemental composition and abundance of the materials can be measured.[149] The detection limit of EDX/EDS is about 0.1 atom-% and the spatial resolution is generally below 1 μm. However, the vertical penetration of the electron beams is generally less than 0.5 μm, which limits the vertical information that can be revealed.[179] X-ray photoelectron spectroscopy works on a similar principle but relies on the detection of the excited electrons from the materials. By measuring the number and the energy of electrons

Table 4. Popular Analytical Techniques for Membrane Physical−Chemical Characterization[58,59,74,86,89,104,196,215−228]

technique	main information	vertical resolution (depth probed, typical)	lateral resolution (typical)	types of solid specimen (typical)	application examples
atomic force microscopy (AFM); scanning force microscopy (SFM)	topographic imaging, friction force, mapping, morphology, profilometry, Elm thickness, wear volume, structure, surface roughness	<0.03 to 0.05 nm	atomic to 1 nm	all kinds of solids	75, 217, 218
auger electron spectroscopy (AES)	elemental composition, chemical state, depth profiling, imaging and mapping	0.5 to 10 nm	a few tens of nm or less	ultrahigh vacuum compatible solids	219, 220
energy-disperse X-ray spectroscopy (EDS); wavelength dispersive X-ray spectroscopy (WDS)	elemental composition ($Z \geq 5$; boron to uranium), spectroscopy, imaging and mapping	0.02 to 1 μm	0.5 to 1 μm for bulk specimens; as small as 1 nm for thin specimens	ultrahigh vacuum compatible solids	221,222
Fourier transform infrared spectroscopy (FTIR)	chemical species'binding, structural inhomogeneity, defects, depth profile	10 nm to μm	20 μm to 5 mm	all kinds of solids	87, 198
Raman spectroscopy	identification of unknown compounds, chemical state, bonding state, structural order, phase transitions, depth profiling	few μm to mm	1 μm	all kinds of solids	223−225
scanning electron microscopy (SEM)	imaging and mapping, morphology, defects	variable from a few nm to a few μm	1 to 50 nm in secondary electron mode	ultrahigh vacuum compatible solids	59, 60, 90
secondary ion mass spectroscopy (SIMS)	chemical strucur/binding, imaging, elemental composition, depth profile	0.3 to 2 nm	10 nm to 2 mm	ultrahigh vacuum compatible solids	226, 227
transmission electron microscopy (TEM)	atomic structure, microstructure, crystallography, structure, defect imaging, morphology, chemical bonding	none	≤0.2 nm	ultrahigh vacuum compatible solids	105, 228
X-ray photoelectron spectroscopy (XPS)	elemental composition, chemical state, depth profiling, imaging and mapping	a few to several nm	5 μm to 5 mm	ultrahigh vacuum compatible solids	226, 229
X-ray diffraction (XRD)	crystalline phases, orientation and size, atomic arrangements, defect imaging, film thickness	a few μm	none; ~10 μm with microfocus	dry solid	220, 230

dx.doi.org/10.1021/ie101928r |Ind. Eng. Chem. Res. 2011, 50, 3798–3817

that escaped from the surface with X-ray irradiation, the elemental composition, empirical formula, chemical state, and electronic state of the elements can be revealed.[149] One advantage of XPS analysis is the low energy incident X-rays, which enables nondestructive examination of the surface.[149,180] The typical analysis depth is 1−3 nm, making XPS a valuable tool to reveal skin layer information. However, both EDX and XPS require the samples to be conductive. Thus, most polymeric membranes have to be coated with conductive material before analysis. Secondary ion mass spectrometry collects and analyzes the ejected secondary ions from the sample surface sputtered by primary ion beams. The secondary ions measured by mass spectrometer can be used to determine the elemental, isotopic, and molecular composition of the membrane. In modern SIMS equipment, the charging of sample can be avoided with electron flood sources. As the primary ion beam can rapidly sputter the surface, SIMS technique is applicable to reveal the depth profile of chemical composition.[157,181]

4.2.3.3. Surface Hydrophilicity and Surface Energy. Membrane hydrophilicity is a very important interfacial property that can be modified by changing phase inversion process conditions or polymer chemistry. The most common method to determine the hydrophilicity of a membrane is the measurement of contact angle. Among the various ways to measure the contact angle, the sessile drop method is the most widely used.[182] Because of surface tension, the surface of any liquid is an interface between that liquid and another medium. Interfacial tension is a property of the liquid's interaction with another medium, e.g., the membrane. Where the two materials meet, the geometry of the interface is determined from the balance of interfacial forces.[183] So, a wealth of information can be obtained through the measurement of the contact angle between the liquid and membrane surface.

One piece of important information that can be obtained by contact angle measurement is the surface free energy of the membrane. Analysis of contact angles of liquid droplets on a solid substrate provide parameters describing Lifshitz−van der Waals, electron-donor, and electron-acceptor components of the solid surface tension.[184,185] The surface tension parameters collectively describe the Lifshitz−van der Waals and Lewis acid−base interfacial free energy (per unit area) of any material immersed in water. Although simple water contact angles suggest a material's "hydrophilicity", the interfacial free energy of cohesion (per unit area) of a given material immersed in water gives an indication of inherent (thermodynamic) stability or aggregation propensity. The more positive the overall free energy of *cohesion*, the more hydrophilic, stable, and resistant to *aggregation* is the material. Alternatively, the free energy of adhesion (per unit area) of two different materials (e.g., a colloidal particle and a sand grain) immersed in water gives an indication of inherent (thermodynamic) stability or deposition propensity. The more positive the overall free energy of *adhesion*, the more hydrophilic, stable, and resistant to *deposition* is the material.

Probe liquids with known surface tensions (such as diiodomethane, glycerol, and water) enable determination of the three surface tension parameters by solving the extended Young equation simultaneously for each liquid.[185,186] The polar (electron-donor/acceptor) components of surface tension both change with subtle variations in aqueous solution chemistry (ionic strength, pH, plurivalent ions, and buffer capacity); hence, one can also record contact angles of various aqueous electrolytes to determine the variation in polar surface tension components.[184,186,187] In addition, contact angles measured for buffered and unbuffered water drops adjusted to different pH values can be used to quantify solid substrate surface charge density and ionization fraction as a function pH.[185,188,189]

4.2.3.4. Surface Roughness. The interaction potentials between membrane surface and particulate matter are also influenced by membrane surface roughness.[190,191] Recent studies indicate that the roughness/morphology of membrane surfaces impacts the magnitudes of interaction potentials to the same extent as similar changes in the magnitudes of chemical free energy and electrostatic interaction.[192,193] Although EM provides fine resolutions of surface topography, the quantitative and statistical analysis of surface roughness features is obtained through AFM measurements.[194] Key parameters describing membrane surface morphology (e.g., mean roughness, average roughness, root-mean-square roughness, surface area difference, peak count per unit area, and the ratio of asperity separation to asperity size) can be obtained through AFM examination.[194]

4.2.3.5. Surface Charge. Most polymers acquire an electric surface charge when brought into contact with an aqueous solution. Once the membrane is brought into contact with an aqueous electrolyte solution, the dissociation of functional groups and adsorption of ions/molecules causes most of the membrane surface to become charged. It has been well recognized that charge or electrical properties of polymeric membranes have a substantial influence on their filtration performances.[195] The surface charge properties of membranes are often characterized by zeta potential, which is the electric potential in the interfacial double layer at the location of the slipping plane versus a point in the bulk fluid away from the interface. Generally, the fundamental equation relating the measured streaming potential to the zeta potential (ζ) is given by the classical Helmholtz−Smoluchowski formula[196]

$$\zeta = \frac{\Delta V}{\Delta P}\frac{\mu \kappa_b}{\varepsilon_r \varepsilon_0} \tag{31}$$

where $\Delta V/\Delta P$ is the streaming potential, ε_0 is the vacuum permittivity, ε_r is the relative dielectric constant of the liquid, μ is the liquid viscosity, and κ_b is the conductivity of the bulk electrolyte. This equation was later modified by Yaroshchuk et al.[197] and experimentally verified by Fievet et al.[198] as

$$\zeta = \frac{\Delta V}{\Delta P}\kappa_t \frac{\mu}{\varepsilon_r \varepsilon_0}\frac{L}{hD} \tag{32}$$

where κ_t is the total conductance of the membrane/channel/membrane system, L is the length of the slit channel, h is the height of the slit channel, and D is the width of the slit channel.

Many methods have been developed to qualitatively and quantitatively characterize membrane surface charge, including streaming potential measurement, impedance spectroscopy, membrane potential measurements, and titration. The obtained zeta potential is a function of material intrinsic properties, such as membrane backbone materials, surface functional groups, and internal structure. Solution chemistries are also proven to have pronounced influence on the zeta potential measurements, such as solution pH, ionic strength, and even ionic composition.

5. CONCLUSIONS

In this Review, a basic description about the preparation and characterization was given for nonsolvent induced phase inversion membranes. Basic formation mechanisms for different

membrane morphologies were introduced. Key factors of the membrane preparation process including the choice of solvent−nonsolvent system, the composition of the polymer solution, the composition of the coagulation bath, the choice of additives in the system, and film casting conditions were discussed. Mechanisms of the system thermodynamics and process kinetics were also discussed. We can predict that membranes with suitable morphology, stability, and permeation properties can be obtained from judging such key factors.

AUTHOR INFORMATION

Corresponding Author

*Address: University of California, Los Angeles; 5732-G Boelter Hall; PO Box 95153; Los Angeles, California, 90095. Tel: (310) 206-3735. Fax: (310) 206-2222. E-mail: emvhoek@ucla.edu.

ACKNOWLEDGMENT

This publication is based on work supported in part by Award No. KUS-C1-018-02, made by King Abdullah University of Science and Technology (KAUST) through the KAUST-Cornell Center for Energy and Sustainability in addition to funding provided by Abraxis Bioscience Inc.

REFERENCES

(1) Crittenden, J. C.; Trussel, R. R.; Hand, D. W.; Howe, K. J.; Tchobanoglous, G. *Water Treatment: Principles and Design*, 2nd ed.; John Wiley & Sons, Inc.: Hoboken, NJ, 2005.

(2) Cheryan, M. *Ultrafiltration and Microfiltration Handbook*; Technomic: Lancaster, PA, 1998.

(3) Mulder, M. *Basic Principles of Membrane Technology*; Kluwer Academic Publishers: Dordrecht, The Netherlands, 2003.

(4) Loeb, G. S.; Sourirajan, S. Sea water demineralization by means of an osmotic membrane. *Adv. Chem. Ser.* **1968**, *38*, 117.

(5) Guillotin, M.; Lemoyne, C.; Noel, C.; Monnerie, L. Physicochemical processes occurring during formation of cellulose diacetate membranes - research of criteria for optimizing membrane performance - 4. Cellulose diacetate-acetone-organic additive casting solutions. *Desalination* **1977**, *21*, 165.

(6) Koenhen, D. M.; Mulder, M. H. V.; Smolders, C. A. Phase separation phenomena during formation of asymmetric membranes. *J. Appl. Polym. Sci.* **1977**, *21*, 199.

(7) Cabasso, I.; Klein, E.; Smith, J. K. Polysulfone hollow fibers. 1. Spinning and properties. *J. Appl. Polym. Sci.* **1976**, *20*, 2377.

(8) Cabasso, I.; Klein, E.; Smith, J. K. Polysulfone hollow fibers. 2. Morphology. *J. Appl. Polym. Sci.* **1977**, *21*, 165.

(9) Sukitpaneenit, P.; Chung, T. S. Molecular elucidation of morphology and mechanical properties of PVDF hollow fiber membranes from aspects of phase inversion, crystallization and rheology. *J. Membr. Sci.* **2009**, *340*, 192.

(10) Koops, G. H.; Nolten, J. A. M.; Mulder, M. H. V.; Smolders, C. A. Integrally skinned polysulfone hollow-fiber membranes for pervaporation. *J. Appl. Polym. Sci.* **1994**, *54*, 385.

(11) Ghosh, A. K.; Jeong, B. H.; Huang, X. F.; Hoek, E. M. V. Impacts of reaction and curing conditions on polyamide composite reverse osmosis membrane properties. *J. Membr. Sci.* **2008**, *311*, 34.

(12) Strathmann, H.; Kock, K. Formation mechanism of phase inversion membranes. *Desalination* **1977**, *21*, 241.

(13) Wijmans, J. G.; Kant, J.; Mulder, M. H. V.; Smolders, C. A. Phase-separation phenomena in solutions of polysulfone in mixtures of a solvent and a nonsolvent - relationship with membrane formation. *Polymer* **1985**, *26*, 1539.

(14) Smolders, C. A.; Reuvers, A. J.; Boom, R. M.; Wienk, I. M. Microstructures in phase-inversion membranes. 1. Formation of macrovoids. *J. Membr. Sci.* **1992**, *73*, 259.

(15) Strathmann, H.; Kock, K.; Amar, P.; Baker, R. W. Formation mechanism of asymmetric membranes. *Desalination* **1975**, *16*, 179.

(16) Cohen, C.; Tanny, G. B.; Prager, S. Diffusion-controlled formation of porous structures in ternary polymer systems. *J. Polym. Sci., Part B: Polym. Phys.* **1979**, *17*, 477.

(17) Reuvers, A. J.; Vandenberg, J. W. A.; Smolders, C. A. Formation of membranes by means of immersion precipitation. 1. A model to describe mass-transfer during immersion precipitation. *J. Membr. Sci.* **1987**, *34*, 45.

(18) Tsay, C. S.; McHugh, A. J. Mass-transfer modeling of asymmetric membrane formation by phase inversion. *J. Polym. Sci., Part B: Polym. Phys.* **1990**, *28*, 1327.

(19) Radovanovic, P.; Thiel, S. W.; Hwang, S. T. Formation of asymmetric polysulfone membranes by immersion precipitation. 1. Modeling mass-transport during gelation. *J. Membr. Sci.* **1992**, *65*, 213.

(20) Radovanovic, P.; Thiel, S. W.; Hwang, S. T. Formation of asymmetric polysulfone membranes by immersion precipitation. 2. The effects of casting solution and gelation bath compositions on membrane-structure and skin formation. *J. Membr. Sci.* **1992**, *65*, 231.

(21) Matz, R. Structure of cellulose-acetate membranes. 1. Development of porous structures in anisotropic membranes. *Desalination* **1972**, *10*, 1.

(22) Frommer, M. A.; Lancet, D. The mechanism of membrane formation: Membrane structures and their relation to preparation conditions. In *Reverse Osmosis Membrane Research*; Lonsdale, H. K., Podall, H. E., Eds.; Plenum Press: New York, 1972.

(23) Ray, R. J.; Krantz, W. B.; Sani, R. L. Linear-stability theory model for finger formation in asymmetric membranes. *J. Membr. Sci.* **1985**, *23*, 155.

(24) Boom, R. M.; Wienk, I. M.; Vandenboomgaard, T.; Smolders, C. A. Microstructures in phase inversion membranes. 2. The role of a polymeric additive. *J. Membr. Sci.* **1992**, *73*, 277.

(25) Kimmerle, K.; Strathmann, H. Analysis of the structure-determining process of phase inversion membranes. *Desalination* **1990**, *79*, 283.

(26) Lai, J. Y.; Lin, F. C.; Wang, C. C.; Wang, D. M. Effect of nonsolvent additives on the porosity and morphology of asymmetric TPX membranes. *J. Membr. Sci.* **1996**, *118*, 49.

(27) Yilmaz, L.; McHugh, A. J. Analysis of nonsolvent solvent polymer phase-diagrams and their relevance to membrane formation modeling. *J. Appl. Polym. Sci.* **1986**, *31*, 997.

(28) Cheng, L. P.; Dwan, A. H.; Gryte, C. C. Membrane formation by isothermal precipitation in polyamide formic-acid water-systems. 1. Description of membrane morphology. *J. Polym. Sci., Part B: Polym. Phys.* **1995**, *33*, 211.

(29) Termonia, Y. Fundamentals of polymer coagulation. *J. Polym. Sci., Part B: Polym. Phys.* **1995**, *33*, 279.

(30) Cheng, J. M.; Wang, D. M.; Lin, F. C.; Lai, J. Y. Formation and gas flux of asymmetric pmma membranes. *J. Membr. Sci.* **1996**, *109*, 93.

(31) Paulsen, F. G.; Shojaie, S. S.; Krantz, W. B. Effect of evaporation step on macrovoid formation in wet-cast polymeric membranes. *J. Membr. Sci.* **1994**, *91*, 265.

(32) Young, T. H.; Cheng, L. P.; Lin, D. J.; Fane, L.; Chuang, W. Y. Mechanisms of PVDF membrane formation by immersion-precipitation in soft (1-octanol) and harsh (water) nonsolvents. *Polymer* **1999**, *40*, 5315.

(33) Li, C. L.; Wang, D. M.; Deratani, A.; Quemener, D.; Bouyer, D.; Lai, J. Y. Insight into the preparation of poly(vinylidene fluoride) membranes by vapor-induced phase separation. *J. Membr. Sci.* **2010**, *361*, 154.

(34) Flory, P. J. Thermodynamics of high polymer solutions. *J. Chem. Phys.* **1941**, *9*, 660.

(35) Huggins, M. L. Solutions of long chain compounds. *J. Chem. Phys.* **1941**, *9*, 440.

(36) Huggins, M. L. Theory of solutions of high polymers. *J. Am. Chem. Soc.* **1942**, *64*, 1712.

(37) Fried, J. *Polymer Science and Technology*; Prentice Hall: Upper Saddle River, NJ, 2003.

(38) Lipson, J. E. G.; Guillet, J. E. In *Developments in Polymer Characterisation*; Dawkins, J. V., Ed.; Applied Science Publishers: London, 1982.
(39) Flory, P. J.; Krigbaum, W. R. Statistical mechanics of dilute polymer solutions. II. *J. Chem. Phys.* **1950**, *18*, 1086.
(40) Koningsveld, R.; Kleintjens, L. A.; Schoffeleers, H. M. Thermodynamic aspects of polymer compatibility. *Pure Appl. Chem.* **1974**, *39*, 1.
(41) Hoy, K. L. New values of solubility parameters from vapor pressure data. *J. Paint Technol.* **1970**, *42*, 76.
(42) Small, P. A. Some factors affecting the solubility of polymers. *J. Appl. Chem.* **1953**, *3*, 71.
(43) van Krevelen, D. W. *Properties of Polymers*; Elsevier: Amsterdam, 1990.
(44) Hildebrand, J. H.; Scott, R. L. *The Solubility of Non-Electrolytes*; Reinhold: New York, 1959.
(45) Scatchard, G. Equilibria in non-electrolyte solutions in relation to the vapor pressures and densities of the components. *Chem. Rev.* **1931**, *8*, 321.
(46) Hansen, C. M. The three dimensional solubility parameter and solvent diffusion coefficient. Ph.D. Thesis, University of Copenhagen, 1967.
(47) Hansen, C. M. Solubility Parameters - An Introduction. In *Hansen Solubility Parameters - A User's Handbook*; CRC Press: Boca Raton, FL, 2000; Chapter 1.
(48) Hansen, C. M.; Beerbower, A., Solubility parameters. In *Kirk-Othmer Encyclopedia of Chemical Technology*; Standen, A., Ed.; Interscience: New York, 1971.
(49) Hansen, C. M. The three dimensional solubility parameter - key to paint component affinities I. *J. Paint Technol.* **1967**, *39*, 104.
(50) Hansen, C. M. The three dimensional solubility parameter - key to paint component affinities II. *J. Paint Technol.* **1967**, *39*, 505.
(51) Hansen, C. M.; Skaarup, K. The three dimensional solubility parameter - key to paint component affinities III. *J. Paint Technol.* **1967**, *39*, 511.
(52) Blanks, R. F.; Prausnitz, J. M. Thermodynamics of polymer solubility in polar + nonpolar systems. *Ind. Eng. Chem. Fundam.* **1964**, *3*, 1.
(53) Hansen, C. M. Methods of Characterization - Polymers. In *Hansen Solubility Parameters - A User's Handbook*; CRC Press: Boca Raton, FL, 2000; Chapter 3.
(54) Hansen, C. M. Appendix. In *Hansen Solubility Parameters - A User's Handbook*; CRC Press: Boca Raton, FL, 2000.
(55) Tsai, H. A.; Li, L. D.; Lee, K. R.; Wang, Y. C.; Li, C. L.; Huang, J.; Lai, J. Y. Effect of surfactant addition on the morphology and pervaporation performance of asymmetric polysulfone membranes. *J. Membr. Sci.* **2000**, *176*, 97.
(56) Tsai, H. A.; Ruaan, R. C.; Wang, D. M.; Lai, J. Y. Effect of temperature and Span series surfactant on the structure of polysulfone membranes. *J. Appl. Polym. Sci.* **2002**, *86*, 166.
(57) Han, M. J.; Nam, S. T. Thermodynamic and rheological variation in polysulfone solution by PVP and its effect in the preparation of phase inversion membrane. *J. Membr. Sci.* **2002**, *202*, 55.
(58) Chakrabarty, B.; Ghoshal, A. K.; Purkait, A. K. Preparation, characterization and performance studies of polysulfone membranes using PVP as an additive. *J. Membr. Sci.* **2008**, *315*, 36.
(59) Chakrabarty, B.; Ghoshal, A. K.; Purkait, M. K. Effect of molecular weight of PEG on membrane morphology and transport properties. *J. Membr. Sci.* **2008**, *309*, 209.
(60) Kim, J. H.; Lee, K. H. Effect of PEG additive on membrane formation by phase inversion. *J. Membr. Sci.* **1998**, *138*, 153.
(61) Zheng, Q. Z.; Wang, P.; Yang, Y. N. Rheological and thermodynamic variation in polysulfone solution by PEG introduction and its effect on kinetics of membrane formation via phase-inversion process. *J. Membr. Sci.* **2006**, *279*, 230.
(62) Ahmad, A. L.; Sarif, M.; Ismail, S. Development of an integrally skinned ultrafiltration membrane for wastewater treatment: Effect of different formulations of PSf/NMP/PVP on flux and rejection. *Desalination* **2005**, *179*, 257.
(63) Han, M. J. Effect of propionic acid in the casting solution on the characteristics of phase inversion polysulfone membranes. *Desalination* **1999**, *121*, 31.
(64) Zheng, Q. Z.; Wang, P.; Yang, Y. N.; Cui, D. J. The relationship between porosity and kinetics parameter of membrane formation in PSF ultrafiltration membrane. *J. Membr. Sci.* **2006**, *286*, 7.
(65) Hou, T. P.; Dong, S. H.; Zheng, L. Y. The study of mechanism of organic additives action in the polysulfone membrane casting solution. *Desalination* **1991**, *83*, 343.
(66) Fontyn, M.; Vantriet, K.; Bijsterbosch, B. H. Surface spectroscopic studies of pristine and fouled membranes. 1. Method development and pristine membrane characterization. *Colloids Surf.* **1991**, *54*, 331.
(67) Barth, C.; Goncalves, M. C.; Pires, A. T. N.; Roeder, J.; Wolf, B. A. Asymmetric polysulfone and polyethersulfone membranes: Effects of thermodynamic conditions during formation on their performance. *J. Membr. Sci.* **2000**, *169*, 287.
(68) Baik, K. J.; Kim, J. Y.; Lee, H. K.; Kim, S. C. Liquid-liquid phase separation in polysulfone/polyethersulfone/N-methyl-2-pyrrolidone/water quaternary system. *J. Appl. Polym. Sci.* **1999**, *74*, 2113.
(69) Chaturvedia, B. K.; Ghosh, A. K.; Ramachandhran, V.; Trivedi, M. K.; Hanra, M. S.; Misra, B. M. Preparation, characterization and performance of polyethersulfone ultrafiltration membranes. *Desalination* **2001**, *133*, 31.
(70) Liu, Y.; Koops, G. H.; Strathmann, H. Characterization of morphology controlled polyethersulfone hollow fiber membranes by the addition of polyethylene glycol to the dope and bore liquid solution. *J. Membr. Sci.* **2003**, *223*, 187.
(71) Mosqueda-Jimenez, D. B.; Narbaitz, R. M.; Matsuura, T.; Chowdhury, G.; Pleizier, G.; Santerre, J. P. Influence of processing conditions on the properties of ultrafiltration membranes. *J. Membr. Sci.* **2004**, *231*, 209.
(72) Hwang, J. R.; Koo, S. H.; Kim, J. H.; Higuchi, A.; Tak, T. M. Effects of casting solution composition on performance of poly(ether sulfone) membrane. *J. Appl. Polym. Sci.* **1996**, *60*, 1343.
(73) Barzin, J.; Sadatnia, B. Theoretical phase diagram calculation and membrane morphology evaluation for water/solvent/polyethersulfone systems. *Polymer* **2007**, *48*, 1620.
(74) Idris, A.; Zain, N. M.; Noordin, M. Y. Synthesis, characterization and performance of asymmetric polyethersulfone (PES) ultrafiltration membranes with polyethylene glycol of different molecular weights as additives. *Desalination* **2007**, *207*, 324.
(75) Li, J. F.; Xu, Z. L.; Yang, H. Microporous polyethersulfone membranes prepared under the combined precipitation conditions with non-solvent additives. *Polym. Adv. Technol.* **2008**, *19*, 251.
(76) Rahimpour, A.; Madaeni, S. S. Polyethersulfone (PES)/cellulose acetate phthalate (CAP) blend ultrafiltration membranes: Preparation, morphology, performance and antifouling properties. *J. Membr. Sci.* **2007**, *305*, 299.
(77) Rahimpour, A.; Madaeni, S. S.; Mansourpanah, Y. High performance polyethersulfone UF membrane for manufacturing spiral wound module: Preparation, morphology, performance, and chemical cleaning. *Polym. Adv. Technol.* **2007**, *18*, 403.
(78) Cornelissen, E. R.; Boomgaard, T.; Strathmann, H. Physicochemical aspects of polymer selection for ultrafiltration and microfiltration membranes. *Colloids Surf., A* **1998**, *138*, 283.
(79) Chandorikar, M. V.; Bhavsar, P. C. Evaluation of polyacrylonitrile and poly(methyl methacrylate) as membrane materials for reverse-osmosis. *Indian J. Technol.* **1983**, *21*, 124.
(80) Belfer, S. Modification of ultrafiltration polyacrylonitrile membranes by sequential grafting of oppositely charged monomers: pH-dependent behavior of the modified membranes. *React. Funct. Polym.* **2003**, *54*, 155.
(81) Kim, I. C.; Yun, H. G.; Lee, K. H. Preparation of asymmetric polyacrylonitrile membrane with small pore size by phase inversion and post-treatment process. *J. Membr. Sci.* **2002**, *199*, 75.
(82) Scharnagl, N.; Buschatz, H. Polyacrylonitrile (PAN) membranes for ultra- and microfiltration. *Desalination* **2001**, *139*, 191.
(83) Musale, D. A.; Kumari, A.; Pleizier, G. Formation and characterization of poly(acrylonitrile)/chitosan composite ultrafiltration membranes. *J. Membr. Sci.* **1999**, *154*, 163.

(84) Zhu, T. R.; Luo, Y. B.; Lin, Y. W.; Li, Q.; Yu, P.; Zeng, M. Study of pervaporation for dehydration of caprolactam through blend NaAlg-poly(vinyl pyrrolidone) membranes on PAN supports. *Sep. Purif. Technol.* **2010**, *74*, 242.

(85) Zhang, G. J.; Meng, H.; Ji, S. L. Hydrolysis differences of polyacrylonitrile support membrane and its influences on polyacrylonitrile-based membrane performance. *Desalination* **2009**, *242*, 313.

(86) Oh, N. W.; Jegal, J.; Lee, K. H. Preparation and characterization of nanofiltration composite membranes using polyacrylonitrile (PAN). I. Preparation and modification of PAN supports. *J. Appl. Polym. Sci.* **2001**, *80*, 1854.

(87) Reddy, A. V. R.; Patel, H. R. Chemically treated polyethersulfone/polyacrylonitrile blend ultrafiltration membranes for better fouling resistance. *Desalination* **2008**, *221*, 318.

(88) Qin, J. J.; Cao, Y. M.; Li, Y. Q.; Li, Y.; Oo, M. H.; Lee, H. W. Hollow fiber ultrafiltration membranes made from blends of PAN and PVP. *Sep. Purif. Technol.* **2004**, *36*, 149.

(89) Yang, S.; Liu, Z. Z. Preparation and characterization of polyacrylonitrile ultrafiltration membranes. *J. Membr. Sci.* **2003**, *222*, 87.

(90) Nouzaki, K.; Nagata, M.; Arai, J.; Idemoto, Y.; Koura, N.; Yanagishita, H.; Negishi, H.; Kitamoto, D.; Ikegami, T.; Haraya, K. Preparation of polyacrylonitrile ultrafiltration membranes for wastewater treatment. *Desalination* **2002**, *144*, 53.

(91) Yang, S.; Liu, Z. Z.; Chen, H. Z. A gas-liquid chemical reaction treatment and phase inversion technique for formation of high permeability pan of membranes. *J. Membr. Sci.* **2005**, *246*, 7.

(92) Matz, R. Structure of cellulose-acetate membranes. 2. Physical and transport characteristics of porous layer of anisotropic membranes. *Desalination* **1972**, *11*, 207.

(93) Arockiasamy, D. L.; Nagendran, A.; Shobana, K. H.; Mohan, D. Preparation and characterization of cellulose acetate/aminated polysulfone blend ultrafiltration membranes and their application studies. *Sep. Sci. Technol.* **2009**, *44*, 398.

(94) Arthanareeswaran, G.; Devi, T. K. S.; Raajenthiren, M. Effect of silica particles on cellulose acetate blend ultrafiltration membranes: Part I. *Sep. Purif. Technol.* **2008**, *64*, 38.

(95) Nagendran, A.; Vidya, S.; Mohan, D. Preparation and characterization of cellulose acetate-sulfonated poly (ether imide) blend ultrafiltration membranes and their applications. *Soft Mater.* **2008**, *6*, 45.

(96) Raguime, J. A.; Arthanareeswaran, G.; Thanikaivelan, P.; Mohan, D.; Raajenthiren, M. Performance characterization of cellulose acetate and poly(vinylpyrrolidone) blend membranes. *J. Appl. Polym. Sci.* **2007**, *104*, 3042.

(97) Arthanareeswaran, G.; Thanikaivelan, P.; Srinivasn, K.; Mohan, D.; Rajendran, M. Synthesis, characterization and thermal studies on cellulose acetate membranes with additive. *Eur. Polym. J.* **2004**, *40*, 2153.

(98) Vidya, S.; Vijayalakshmi, A.; Nagendran, A.; Mohan, D. Effect of additive concentration on cellulose acetate blend membranes-preparation, characterization and application studies. *Sep. Sci. Technol.* **2008**, *43*, 1933.

(99) Malaisamy, R.; Mahendran, R.; Mohan, D.; Rajendran, M.; Mohan, V. Cellulose acetate and sulfonated polysulfone blend ultrafiltration membranes. I. Preparation and characterization. *J. Appl. Polym. Sci.* **2002**, *86*, 1749.

(100) Fujiwara, N.; Fukuda, T.; Yanaga, Y.; Sekino, M.; Goto, T. The reference and analysis of a double-element type hollow-fiber RO module in seawater desalination. *Desalination* **1994**, *96*, 441.

(101) Elguera, A. M.; Nunez, A.; Nishida, M. Experimental test of TOYOBO membranes for seawater desalination at Las Palmas, Spain. *Desalination* **1999**, *125*, 55.

(102) Yoo, S. H.; Jho, J. Y.; Won, J.; Park, H. C.; Kang, Y. S. Effect of solvent and cosolvent on the morphology and permeance of asymmetric polyimide membrane. *J. Ind. Eng. Chem.* **2000**, *6*, 129.

(103) Yoo, S. H.; Kim, J. H.; Jho, J. Y.; Won, J.; Kang, Y. S. Influence of the addition of PVP on the morphology of asymmetric polyimide phase inversion membranes: Effect of PVP molecular weight. *J. Membr. Sci.* **2004**, *236*, 203.

(104) Perez, S.; Merlen, E.; Robert, E.; Addad, J. P. C.; Viallat, A. Characterization of the surface-layer of integrally skinned polyimide membranes - relationship with their mechanism of formation. *J. Appl. Polym. Sci.* **1993**, *47*, 1621.

(105) Jeon, J. Y.; Tak, T. M. Preparation of newly asymmetric polyimide membranes by phase inversion. *J. Appl. Polym. Sci.* **1996**, *61*, 2345.

(106) Blais, P., Polyamide membranes. In *Reverse osmosis and synthetic membranes: Theory-technology-engineering*; Sourirajan, S., Ed.; National Research Council of Canada: Ottawa, 1977.

(107) Zeni, M.; Riveros, R.; de Souza, J. F.; Mello, K.; Meireles, C.; Rodrigues, G. Morphologic analysis of porous polyamide 6,6 membranes prepared by phase inversion. *Desalination* **2008**, *221*, 294.

(108) Dey, T. K.; Misra, B. M. Characteristic properties of a few selected polymers for reverse osmosis applications. *J. Polym. Mater.* **1999**, *16*, 13.

(109) Zuo, D. Y.; Xu, Y. Y.; Xu, W. L.; Zou, H. T. The influence of PEG molecular weight on morphologies and properties of pvdf asymmetric membranes. *Chin. J. Polym. Sci.* **2008**, *26*, 405.

(110) Wu, B.; Li, K.; Te, W. K. Preparation and characterization of poly(vinylidene fluoride) hollow fiber membranes for vacuum membrane distillation. *J. Appl. Polym. Sci.* **2007**, *106*, 1482.

(111) Wang, D. L.; Li, K.; Teo, W. K. Preparation and characterization of polyvinylidene fluoride (PVDF) hollow fiber membranes. *J. Membr. Sci.* **1999**, *163*, 211.

(112) Hou, D. Y.; Wang, J.; Qu, D.; Luan, Z. K.; Zhao, C. W.; Ren, X. J. Preparation of hydrophobic PVDF hollow fiber membranes for desalination through membrane distillation. *Water Sci. Technol.* **2009**, *59*, 1219.

(113) Zhang, Z. L.; Chen, S. M. SEM study on the morphological structure of PTFE stretching porous membranes - SEM identification for PTFE stretching porous membranes in preparation. *Chin. J. Chem. Phys.* **2003**, *16*, 151.

(114) Kang, K.; Kang, P. H.; Nho, Y. C. Preparation and characterization of a proton-exchange membrane by the radiation grafting of styrene onto polytetrafluoroethylene films. *J. Appl. Polym. Sci.* **2006**, *99*, 1415.

(115) Choi, S. H.; Tasselli, F.; Jansen, J. C.; Barbieri, G.; Drioli, E. Effect of the preparation conditions on the formation of asymmetric poly(vinylidene fluoride) hollow fibre membranes with a dense skin. *Eur. Polym. J.* **2010**, *46*, 1713.

(116) Baker, R. W. *Membrane Technology and Applications*; John Wiley & Sons, Ltd.: New York, 2004.

(117) Han, M. J.; Bhattacharyya, D. Morphology and transport study of phase inversion polysulfone membranes. *Chem. Eng. Commun.* **1994**, *128*, 197.

(118) Kang, Y. S.; Kim, H. J.; Kim, U. Y. Asymmetric membrane formation via immersion precipitation method. 1. Kinetic effect. *J. Membr. Sci.* **1991**, *60*, 219.

(119) Chen, L. W.; Young, T. H. Effect of nonsolvents on the mechanism of wet-casting membrane formation from EVAL copolymers. *J. Membr. Sci.* **1991**, *59*, 15.

(120) Nechifor, G.; Popescu, G. Asymmetric membranes prepared by immersion-precipitation technique. *Rev. Roum. Chim.* **1990**, *35*, 899.

(121) Chun, K. Y.; Jang, S. H.; Kim, H. S.; Kim, Y. W.; Han, H. S.; Joe, Y. I. Effects of solvent on the pore formation in asymmetric 6FDA-4,4′ ODA polyimide membrane: Terms of thermodynamics, precipitation kinetics, and physical factors. *J. Membr. Sci.* **2000**, *169*, 197.

(122) Oh, S. J.; Kim, N.; Lee, Y. T. Preparation and characterization of PVDF/TiO_2 organic-inorganic composite membranes for fouling resistance improvement. *J. Membr. Sci.* **2009**, *345*, 13.

(123) Boom, R. M.; Vandenboomgaard, T.; Smolders, C. A. Mass-transfer and thermodynamics during immersion precipitation for a 2-polymer system - evaluation with the system PES-PVP-NMP-water. *J. Membr. Sci.* **1994**, *90*, 231.

(124) Wienk, I. M.; Boom, R. M.; Beerlage, M. A. M.; Bulte, A. M. W.; Smolders, C. A.; Strathmann, H. Recent advances in the formation of phase inversion membranes made from amorphous or semi-crystalline polymers. *J. Membr. Sci.* **1996**, *113*, 361.

(125) Wan, L. S.; Xu, Z. K.; Wang, Z. G. Leaching of PVP from polyacrylonitrile/PVP blending membranes: A comparative study of asymmetric and dense membranes. *J. Polym. Sci., Part B: Polym. Phys.* **2006**, *44*, 1490.

(126) Matsuyama, H.; Maki, T.; Teramoto, M.; Kobayashi, K. Effect of PVP additive on porous polysulfone membrane formation by immersion precipitation method. *Sep. Sci. Technol.* **2003**, *38*, 3449.

(127) Jung, B.; Yoon, J. K.; Kim, B.; Rhee, H. W. Effect of molecular weight of polymeric additives on formation, permeation properties and hypochlorite treatment of asymmetric polyacrylonitrile membranes. *J. Membr. Sci.* **2004**, *243*, 45.

(128) Yuan, Z.; Xi, D. L. Effect of PVP additive on PVDF/TPU blend hollow fibre membranes by phase inversion. *Iran. Polym. J.* **2007**, *16*, 241.

(129) Saljoughi, E.; Amirilargani, M.; Mohammadi, T. Effect of poly(vinyl pyrrolidone) concentration and coagulation bath temperature on the morphology, permeability, and thermal stability of asymmetric cellulose acetate membranes. *J. Appl. Polym. Sci.* **2009**, *111*, 2537.

(130) Miyano, T.; Matsuura, T.; Sourirajan, S. Effect of polyvinylpyrrolidone additive on the pore-size and the pore-size distribution of polyethersulfone (Victrex) membranes. *Chem. Eng. Commun.* **1993**, *119*, 23.

(131) Yeo, H. T.; Lee, S. T.; Han, M. J. Role of a polymer additive in casting solution in preparation of phase inversion polysulfone membranes. *J. Chem. Eng. Jpn.* **2000**, *33*, 180.

(132) Torrestiana-Sanchez, B.; Ortiz-Basurto, R. I.; Brito-De La Fuente, E. Effect of nonsolvents on properties of spinning solutions and polyethersulfone hollow fiber ultrafiltration membranes. *J. Membr. Sci.* **1999**, *152*, 19.

(133) Kim, I. C.; Lee, K. H. Effect of poly(ethylene glycol) 200 on the formation of a polyetherimide asymmetric membrane and its performance in aqueous solvent mixture permeation. *J. Membr. Sci.* **2004**, *230*, 183.

(134) Shieh, J. J.; Chung, T. S.; Wang, R.; Srinivasan, M. P.; Paul, D. R. Gas separation performance of poly(4-vinylpyridine)/polyetherimide composite hollow fibers. *J. Membr. Sci.* **2001**, *182*, 111.

(135) Deniz, S. Characteristics of polycarbonate membranes with polyethylene glycol prepared via dry/wet-phase inversion methods. *Desalination* **2006**, *200*, 42.

(136) Fritzsche, A. K.; Cruse, C. A.; Kesting, R. E.; Murphy, M. K. Polysulfone hollow fiber membranes spun from lewis acid - base complexes. 2. The effect of lewis acid to base ratio on membrane-structure. *J. Appl. Polym. Sci.* **1990**, *39*, 1949.

(137) Laninovic, V. Structure of flat sheet membranes obtained from the system polyethersulfone-dimethylacetamide-nonsolvent additive-water. *Polym. Sci., Ser. A* **2005**, *47*, 744.

(138) Lin, F. C.; Wang, D. M.; Lai, C. L.; Lai, J. Y. Effect of surfactants on the structure of PMMA membranes. *J. Membr. Sci.* **1997**, *123*, 281.

(139) Lai, J. Y.; Lin, F. C.; Wu, T. T.; Wang, D. M. On the formation of macrovoids in PMMA membranes. *J. Membr. Sci.* **1999**, *155*, 31.

(140) Wang, D. M.; Lin, F. C.; Wu, T. T.; Lai, J. Y. Formation mechanism of the macrovoids induced by surfactant additives. *J. Membr. Sci.* **1998**, *142*, 191.

(141) Tsai, H. A.; Huang, D. H.; Fan, S. C.; Wang, Y. C.; Li, C. L.; Lee, K. R.; Lai, J. Y. Investigation of surfactant addition effect on the vapor permeation of aqueous ethanol mixtures through polysulfone hollow fiber membranes. *J. Membr. Sci.* **2002**, *198*, 245.

(142) Tsai, H. A.; Huang, D. H.; Ruaan, R. C.; Lai, J. Y. Mechanical properties of asymmetric polysulfone membranes containing surfactant as additives. *J. Ind. Eng. Chem. Res.* **2001**, *40*, 5917.

(143) Kim, I. C.; Lee, K. H.; Tak, T. M. Preparation and characterization of integrally skinned uncharged polyetherimide asymmetric nanofiltration membrane. *J. Membr. Sci.* **2001**, *183*, 235.

(144) Chen, S. H.; Liou, R. M.; Lai, J. Y.; Lai, C. L. Effect of the polarity of additional solvent on membrane formation in polysulfone/N-methyl-2pyrrolidone/water ternary system. *Eur. Polym. J.* **2007**, *43*, 3997.

(145) Alexandre, M.; Dubois, P. Polymer-layered silicate nanocomposites: Preparation, properties and uses of a new class of materials. *Mater. Sci. Eng., R.* **2000**, *28*, 1.

(146) Rong, M. Z.; Zhang, M. Q.; Zheng, Y. X.; Zeng, H. M.; Walter, R.; Friedrich, K. Structure-property relationships of irradiation grafted nano-inorganic particle filled polypropylene composites. *Polymer* **2001**, *42*, 167.

(147) von Werne, T.; Patten, T. E. Preparation of structurally well-defined polymer-nanoparticle hybrids with controlled/living radical polymerizations. *J. Am. Chem. Soc.* **1999**, *121*, 7409.

(148) Reynaud, E.; Gauthier, C.; Perez, J. Nanophases in polymers. *Rev. Metall. (Paris)* **1999**, *96*, 169.

(149) Wiesner, M.; Bottero, J.-Y. *Environmental Nanotechnology: Applications and Impacts of Nanomaterials*; McGraw-Hill Professional: New York, 2007.

(150) Calvert, P. Potential applications of nanotubes. In *Carbon Nanotubes - Preparation and Properties*; Ebbesen, T. W., Ed.; CRC Press: Boca Raton, FL, 1997.

(151) Favier, V.; Canova, G. R.; Shrivastava, S. C.; Cavaille, J. Y. Mechanical percolation in cellulose whisker nanocomposites. *Polym. Eng. Sci.* **1997**, *37*, 1732.

(152) Chazeau, L.; Cavaille, J. Y.; Canova, G.; Dendievel, R.; Boutherin, B. Viscoelastic properties of plasticized pvc reinforced with cellulose whiskers. *J. Appl. Polym. Sci.* **1999**, *71*, 1797.

(153) Kulprathipanja, S.; Neuzil, R. W.; Li, N. *Separation of gases by means of mixed matrix membranes*. US Patent 4740219, 26 April, 1988.

(154) Jia, M. D.; Peinemann, K. V.; Behling, R. D. Molecular-sieving effect of the zeolite-filled silicone-rubber membranes in gas permeation. *J. Membr. Sci.* **1991**, *57*, 289.

(155) Wang, X. Y.; Zhang, L.; Sun, D. H.; An, Q. F.; Chen, H. L. Effect of coagulation bath temperature on formation mechanism of poly-(vinylidene fluoride) membrane. *J. Appl. Polym. Sci.* **2008**, *110*, 1656.

(156) Yang, Y. N.; Zhang, H. X.; Wang, P.; Zhang, M. Y.; Yang, H. D.; Hu, M. Z.; Jin, J. Kinetic and thermodynamic research of polysulfone/TiO_2 hybrid ultrafiltration membrane. *Acta. Chim. Sin.* **2007**, *65*, 1258.

(157) Li, N. N.; Fane, A. G.; Ho, W. S. W.; Matsuura, T. *Advanced Membrane Technology and Applications*; John Wiley & Sons, Inc.: Hoboken, NJ, 2008.

(158) Wang, D. M.; Lin, F. C.; Chiang, J. C.; Lai, J. Y. Control of the porosity of asymmetric TPX membranes. *J. Membr. Sci.* **1998**, *141*, 1.

(159) Strathmann, H.; Scheible, P. Formation mechanism of asymmetrical cellulose acetate membranes. *Kolloid Z. Z. Polym.* **1971**, *246*, 669.

(160) Lau, W. W. Y.; Guiver, M. D.; Matsuura, T. Phase-separation in polysulfone solvent water and polyethersulfone solvent water-systems. *J. Membr. Sci.* **1991**, *59*, 219.

(161) Wyart, Y.; Georges, G.; Demie, C.; Amra, C.; Moulin, P. Membrane characterization by microscopic methods: Multiscale structure. *J. Membr. Sci.* **2008**, *315*, 82.

(162) Nakao, S. Determination of pore-size and pore-size distribution. 3. Filtration membranes. *J. Membr. Sci.* **1994**, *96*, 131.

(163) Zhao, C. S.; Zhou, X. S.; Yue, Y. L. Determination of pore size and pore size distribution on the surface of hollow-fiber filtration membranes: A review of methods. *Desalination* **2000**, *129*, 107.

(164) Powers, K. W.; Brown, S. C.; Krishna, V. B.; Wasdo, S. C.; Moudgil, B. M.; Roberts, S. M. Research strategies for safety evaluation of nanomaterials. Part VI. Characterization of nanoscale particles for toxicological evaluation. *Toxicol. Sci.* **2006**, *90*, 296.

(165) Abaticchio, P.; Bottino, A.; Roda, G. C.; Capannelli, G.; Munari, S. Characterization of ultrafiltration polymeric membranes. *Desalination* **1990**, *78*, 235.

(166) Cao, G. Z.; Meijerink, J.; Brinkman, H. W.; Burggraaf, A. J. Permporometry study on the size distribution of active pores in porous ceramic membranes. *J. Membr. Sci.* **1993**, *83*, 221.

(167) Cuperus, F. P.; Bargeman, D.; Smolders, C. A. Permporometry - the determination of the size distribution of active pores in UF membranes. *J. Membr. Sci.* **1992**, *71*, 57.

(168) Calvo, J. I.; Hernandez, A.; Pradanos, P.; Martinez, L.; Bowen, W. R. Pore size distributions in microporous membranes. 2. Bulk characterization of track-etched filters by air porometry and mercury porosimetry. *J. Colloid Interface Sci.* **1995**, *176*, 467.

(169) Barrett, E. P.; Joyner, L. G.; Halenda, P. P. The determination of pore volume and area distributions in porous substances. 1. Computations from nitrogen isotherms. *J. Am. Chem. Soc.* **1951**, *73*, 373.
(170) Brun, M.; Lallemand, A.; Quinson, J. F.; Eyraud, C. New method for simultaneous determination of size and shape of pores - thermoporometry. *Thermochim. Acta* **1977**, *21*, 59.
(171) Quinson, J. F.; Mameri, N.; Guihard, L.; Bariou, B. The study of the swelling of an ultrafiltration membrane under the influence of solvents by thermoporometry and measurement of permeability. *J. Membr. Sci.* **1991**, *58*, 191.
(172) Cuperus, F. P.; Bargeman, D.; Smolders, C. A. Critical-points in the analysis of membrane pore structures by thermoporometry. *J. Membr. Sci.* **1992**, *66*, 45.
(173) Meymarom, A.; Katz, M. G. Measurement of active pore-size distribution of microporous membranes - a new approach. *J. Membr. Sci.* **1986**, *27*, 119.
(174) Miyoshi, K. *Surface Characterization Techniques: An Overview*; Glenn Research Center: Cleveland, 2002.
(175) Kang, S.; Elimelech, M. Bioinspired single bacterial cell force spectroscopy. *Langmuir* **2009**, *25*, 9656.
(176) Bowen, W. R.; Doneva, T. A. Artefacts in AFM studies of membranes: Correcting pore images using fast fourier transform filtering. *J. Membr. Sci.* **2000**, *171*, 141.
(177) Boccaccio, T.; Bottino, A.; Capannelli, G.; Piaggio, P. Characterization of PVDF membranes by vibrational spectroscopy. *J. Membr. Sci.* **2002**, *210*, 315.
(178) Kim, K. J.; Fane, A. G.; Nystrom, M.; Pihlajamaki, A. Chemical and electrical characterization of virgin and protein-fouled polycarbonate track-etched membranes by FTIR and streaming-potential measurements. *J. Membr. Sci.* **1997**, *134*, 199.
(179) Holmbom, B.; Stenius, P. Analytical methods. In *Forest Products Chemistry*; Stenius, P., Ed.; Fapet Oy: Jyväskylä, 2000.
(180) Fulghum, J. E. Recent developments in high energy and spatial resolution analysis of polymers by XPS. *J. Electron.* **1999**, *100*, 331.
(181) Garbassi, F.; Morra, M.; Occhiello, E. *Polymer Surfaces: From Physics to Technology*; Rev Upd Su ed.; Wiley: New York, 1998.
(182) Adamson, A. W. *Physical Chemistry of Surfaces*; John Wiley & Sons, Inc: New York, 2007.
(183) de Gennes, P.-G.; Brochard-Wyart, F.; Quéré, D. *Capillary and Wetting Phenomena–Drops, Bubbles, Pearls, Waves*; Springer: New York, 2002.
(184) Mirza, M.; Guo, Y.; Arnold, K.; van Oss, C. J.; Ohki, S. Hydrophobizing effect of cations on acidic phospholipid membranes. *J. Dispersion Sci. Technol.* **1998**, *19*, 951.
(185) Hurwitz, G.; Guillen, G. R.; Hoek, E. M. V. Probing polyamide membrane surface charge, zeta potential, wettability, and hydrophilicity with contact angle measurements. *J. Membr. Sci.* **2010**, *349*, 349.
(186) Butkus, M. A.; Grasso, D. Impact of aqueous electrolytes on interfacial energy. *J. Colloid Interface Sci.* **1998**, *200*, 172.
(187) van Oss, C. J.; Giese, R. F.; Docoslis, A. Hyperhydrophobicity of the water-air interface. *J. Dispersion Sci. Technol.* **2005**, *26*, 585.
(188) Whitesides, G. M.; Biebuyck, H. A.; Folkers, J. P.; Prime, K. L. Acid-base interactions in wetting. *J. Adhes. Sci. Technol.* **1991**, *5*, 57.
(189) Wamser, C. C.; Gilbert, M. I. Detection of surface functional-group asymmetry in interfacially-polymerized films by contact-angle titrations. *Langmuir* **1992**, *8*, 1608.
(190) Bhattacharjee, S.; Ko, C. H.; Elimelech, M. DLVO interaction between rough surfaces. *Langmuir* **1998**, *14*, 3365.
(191) Wolansky, G.; Marmur, A. The actual contact angle on a heterogeneous rough surface in three dimensions. *Langmuir* **1998**, *14*, 5292.
(192) Huang, X. F.; Bhattacharjee, S.; Hoek, E. M. V. Is surface roughness a "scapegoat" or a primary factor when defining particle-substrate interactions?. *Langmuir* **2010**, *26*, 2528.
(193) Hoek, E. M. V.; Agarwal, G. K. Extended DLVO interactions between spherical particles and rough surfaces. *J. Colloid Interface Sci.* **2006**, *298*, 50.
(194) Hoek, E. M. V.; Bhattacharjee, S.; Elimelech, M. Effect of membrane surface roughness on colloid-membrane DLVO interactions. *Langmuir* **2003**, *19*, 4836.
(195) Fievet, P.; Sbai, M.; Szymczyk, A.; Vidonne, A. Determining the zeta-potential of plane membranes from tangential streaming potential measurements: Effect of the membrane body conductance. *J. Membr. Sci.* **2006**, *281*, 757.
(196) Wang, M.; Wu, L. G.; Zheng, X. C.; Mo, J. X.; Gao, C. J. Surface modification of phenolphthalein poly(ether sulfone) ultrafiltration membranes by blending with acrylonitrile-based copolymer containing ionic groups for imparting surface electrical properties. *J. Colloid Interface Sci.* **2006**, *300*, 286.
(197) Yaroshchuk, A.; Ribitsch, V. Role of channel wall conductance in the determination of zeta-potential from electrokinetic measurements. *Langmuir* **2002**, *18*, 2036.
(198) Fievet, P.; Sbai, M.; Szymczyk, A.; Vidonne, A. Determining the zeta-potential of plane membranes from tangential streaming potential measurements: Effect of the membrane body conductance. *J. Membr. Sci.* **2003**, *226*, 227.
(199) Belfort, G.; Davis, R. H.; Zydney, A. L. The behavior of suspensions and macromolecular solutions in cross-flow microfiltration. *J. Membr. Sci.* **1994**, *96*, 1.
(200) Mir, L.; Michaels, S. L.; Goel, V.; Kaiser, R. Crossflow microfiltration: Applications, design and cost. In *Membrane Handbook*; Ho, W. S. W., Sirkar, K. K., Eds.; Van Nostrand Reinhold: New York, 1992.
(201) Zeman, L. J.; Zydney, A. L. *Microfiltration and Ultrafiltration-Principles and Applications*; Marcel Dekker, Inc.: New York, 1996.
(202) Porter, M. C. Microfiltration. In *Synthetic Membrane: Science, Engineering and Applications*; Bungay, P. M., Lonsdale, H. K., de Pinho, M. N., Eds.; Reidel Publishing Company: Boston, 1986.
(203) Eykamp, W. Microfiltration and ultrafiltration. In *Membrane Separation Technology- Principles and Applications*; Nobel, R. D., Stern, S. A., Eds.; Elsevier: Amsterdam, 1995.
(204) Lonsdale, H. K. Reverse osmosis. In *Synthetic Membrane: Science, Engineering and Applications*; Bungay, P. M., Lonsdal, H. K., Pinho, M. N., Eds.; Reidel Publishing Company: Boston, 1986.
(205) Fell, C. J. D. Reverse osmosis. In *Membrane Separation Technology- Principles and Applications*; Noble, R. D., Stern, S. A., Eds.; Elsevier: Amsterdam, 1995.
(206) Wijmans, J. G.; Baker, R. W.; Athayde, A. L. Pervaporation: Removal of organics from water and organic/organic separations. In *Membrane Processes in Separation and Purification*; Crespo, J. G., Boddeker, K. W., Eds.; Kluwer Academic Publishers: Dordrecht, The Netherlands, 1994.
(207) Amjad, Z. *Reverse Osmosis: Membrane Technology, Water Chemistry, and Industrial Applications*; Van Nostrand Reinhold: New York, 1993.
(208) Paul, D. R.; Yampolskii, Y. *Polymeric Gas Separation Membranes*; CRC Press: London, 1994.
(209) Toshima, N. *Polymer for Gas Separation*; VCH: Weinheim, Germany, 1991.
(210) Huang, R. Y. M. *Pervaporation Membrane Separation Processes*; Elsevier: Amsterdam, 1991.
(211) Eustache, H.; Histi, G. Separation of aqueous organic mixtures by pervaporation and analysis by mass-spectrometry or a coupled gas chromatograph-mass spectrometer. *J. Membr. Sci.* **1981**, *8*, 105.
(212) Moonen, H.; Niefind, H. J. Alcohol reduction in beer by means of dialysis. *Desalination* **1982**, *41*, 327.
(213) Schneider, K.; Vangassel, T. J. Membrane distillation. *Chem. Ing. Tech.* **1984**, *56*, 514.
(214) Cath, T. Y.; Childress, A. E.; Elimelech, M. Forward osmosis: Principles, applications, and recent developments. *J. Membr. Sci.* **2006**, *281*, 70.
(215) Ochoa, N. A.; Pradanos, P.; Palacio, L.; Pagliero, C.; Marchese, J.; Hernandez, A. Pore size distributions based on AFM imaging and retention of multidisperse polymer solutes - characterisation of polyethersulfone UF membranes with dopes containing different PVP. *J. Membr. Sci.* **2001**, *187*, 227.
(216) Fan, Z. F.; Wang, Z.; Sun, N.; Wang, J. X.; Wang, S. C. Performance improvement of polysulfone ultrafiltration membrane by blending with polyaniline nanofibers. *J. Membr. Sci.* **2008**, *320*, 363.

(217) Chen, Y. L.; Zhu, G. S.; Peng, Y.; Yao, X. D.; Qiu, S. L. Synthesis and characterization of (*h0l*) oriented high-silica zeolite beta membrane. *Microporous Mesoporous Mater.* **2009**, *124*, 8.

(218) Yang, J. Y.; Nishimura, C.; Komaki, M. Preparation and characterization of Pd-Cu/V-15Ni composite membrane for hydrogen permeation. *J. Alloys Compd.* **2007**, *431*, 180.

(219) Benavente, J.; Oleinikova, M.; Munoz, M.; Valiente, M. Characterization of novel activated composite membranes by impedance spectroscopy. *J. Electroanal. Chem.* **1998**, *451*, 173.

(220) Campos, E. A.; Gushikem, Y. Composite membrane of niobium(V) oxide and cellulose acetate: Preparation and characterization. *J. Colloid Interface Sci.* **1997**, *193*, 121.

(221) Kim, H. J.; Tabe-Mohammadi, A.; Kumar, A.; Fouda, A. E. Asymmetric membranes by a two-stage gelation technique for gas separation: Formation and characterization. *J. Membr. Sci.* **1999**, *161*, 229.

(222) Bottino, A.; Capannelli, G.; D'Asti, V.; Piaggio, P. Preparation and properties of novel organic-inorganic porous membranes. *Sep. Purif. Technol.* **2001**, *22*−*23*, 269.

(223) Khulbe, K. C.; Matsuura, T. Characterization of synthetic membranes by Raman spectroscopy, electron spin resonance, and atomic force microscopy; a review. *Polymer* **2000**, *41*, 1917.

(224) Wei, J.; Helm, G. S.; Corner-Walker, N.; Hou, X. L. Characterization of a non-fouling ultrafiltration membrane. *Desalination* **2006**, *192*, 252.

(225) Saito, N.; Yamashita, S. Characterization of surface-charge-mosaic-modified ultrafiltration membranes prepared by laser-induced surface graft polymerization. *J. Appl. Polym. Sci.* **1998**, *67*, 1141.

(226) Kazama, S.; Sakashita, M. Gas separation properties and morphology of asymmetric hollow fiber membranes made from cardo polyamide. *J. Membr. Sci.* **2004**, *243*, 59.

(227) Ferjani, E.; Mejdoub, M.; Roudesli, M. S.; Chehimi, M. M.; Picard, D.; Delamar, M. XPS characterization of poly(methylhydrosiloxane)-modified cellulose diacetate membranes. *J. Membr. Sci.* **2000**, *165*, 125.

(228) Yang, Y. N.; Zhang, H. X.; Wang, P.; Zheng, Q. Z.; Li, J. The influence of nano-sized TiO_2 fillers on the morphologies and properties of PSF UF membrane. *J. Membr. Sci.* **2007**, *288*, 231.